Energy 227 (2021) 120471

Contents lists available at ScienceDirect

Energy

journal homepage: www.elsevier.com/locate/energy

A multi-objective formulation of improving flexibility in the operation of electric power systems: Application to mitigation measures during the coronavirus pandemic

Gonzalo E. Alvarez

INGAR/CONICET-UTN, Instituto de Desarrollo y Diseño, Santa Fe, Argentina

ARTICLE INFO

Article history:
Received 15 October 2020
Received in revised form
2 March 2021
Accepted 24 March 2021
Available online 29 March 2021

Keywords:
Electric power system
COVID-19
Energy management strategies
Impact of infection cases

ABSTRACT

The coronavirus pandemic has infected more than 23 million people worldwide by August 2020 along with more than 800,000 deaths. To face this pandemic, a joint effort among different areas has been required. In this context, the correct supply of basic services is the key to enhance the complex circumstance. The operation of the electric power systems is needed to ensure the answer to the situation. Basic services in areas of health, security, food, and communications depend on the electricity supply. Consequently, this paper introduces a multi-objective procedure that enhances the operations of power systems under these circumstances. It considers geographical areas that are affected by coronavirus cases and their effects on the personnel of power plants. To obtain the best combinations of total cost and protection of the workers, lexicographic optimization is implemented. The effectiveness of this approach is studied by solving two test cases: a 6-bus system and the Argentine Electric System with real data about the infection cases. The effects on the electricity generation and transportation stages are studied. The results allow identifying critical areas and proposing corrective actions. The method can reach feasible solutions with a low computational requirement.

1. Introduction

The quick spread of *Severe Acute Respiratory Syndrome Coronavirus 2* (SARS-CoV-2) has resulted in a pandemic of Coronavirus 2019 (COVID-19), as the WHO mentioned in their speeches on March 11 of 2020. The main strategies have been the closure of several industries/businesses, social distancing, and restrictions in non-essential professions. However, despite the adopted measures, the spread of SARS-CoV-2 has continued. This caused collapses in public health in many countries [1], along with the loss of millions of jobs [2]. Confronted with an exceptional situation as this, health and other essential sectors are highly dependent on the normal functioning of the electric power systems. A failure in the electricity supply could leave hospitals and other vital services unable to respond to human needs.

Given the importance of power systems during sensitive situations such as pandemics, it is imperative to study the impact of demand changes that certain phenomena cause in these systems. Some studies can be observed in the literature, such as [3] that studies the changes in power systems observed in different consumption scenarios. The impact responds to different scenarios based on changes in energy storage systems. In Ref. [4], the authors study the impact that the seasonal tariff produce in the population demand. The authors of [5] use statistical downscaling techniques produced by two general circulation models, which study variations in demand in California. In Ref. [6] variations in consumption in Turkey due to changes in policies regarding carbon emissions are studied. Authors apply an augmented form of causality analysis by Granger. In Ref. [7], the author studies changes in demand in Australia due to climate change by using linear regressions. However, the previously mentioned works deal with changes in demand due to reasons that are gradually produced in the long term, such as climate change or energy policies. By contrast, it is difficult to find works that consider changes in the electricity sector that happen suddenly during a pandemic. Although there are works such as [8], where big data techniques are implemented to develop actions that reduce the transmission of COVID-19. However, this works has nothing to do with the behavior of electric power systems.

E-mail addresses: galvarez@santafe-conicet.gov.ar, gonzaloe_alvarez@yahoo.com.ar.

https://doi.org/10.1016/j.energy.2021.120471
0360-5442/

Nomenclature

Indexes

i	Unit index
t	Time index
c	Load index
l	Transmission line
b_i/b_o	Input/output bus
q	Objective function index

Constants

$ld_{c,t}$	Load (MW)
ϑ_t	Cost of not covered demand (USD/MW)
$p_{i,t}^{max}/p_{i,t}^{min}$	Maximum/minimum output (MW)
R_t	Spinning reserve(MW)
I	Total number of units
T	Programing horizon
eps	A sufficient small positive number ($10^{-3} \leq eps \leq 10^{-6}$)
r_p	range of the p^{th} objective function
$\gamma_{i,t}^{pv}$	PV matrix [0,1]
$\gamma_{i,t}^{w}$	Wind forecast (MW)
Pr_i^n	Nuclear rated power (MW)
x_l	Line reactance (p.u.)
pw_i	Amount of MWh that can be produced with each available worker
T_i^{ini}	Number of hours that the unit has been working (if it is positive) or resting (if it is negative)
TW^{ini}	Number of hours during the employees that operate the unit have been working (if it is positive) or resting (if it is negative)
TW_i	/ TR_i Number of hours which employees must remain working/rest

Variables

$p_{i,t}^{g}/p_{i,t}^{ng}/p_{i,t}^{h}/\ p_{i,t}^{n}/p_{i,t}^{w}/p_{i,t}^{pv}/p_{i,t}^{r}$	Power output of unit that works with natural gas/non natural gas/hydro/nuclear/ wind/PV/and rest of renewables (MW)
ncl_t	Not covered demand (MW)
$p\_l_{l,t}$	Line power flow (MW)
$\theta_{b_i,t}$	Bus voltage angle
$w_{i,t}$	amount of personnel required to operate a generator
$z_{i,t}$	Binary status variable relating available workers
s_q	Slack or surplus variable of the q^{th} objective function

Besides, the aforementioned works do not consider a problem, very common during a pandemic, which is the reduction of essential staff due to infections [9]. These problems are especially located in regions with high levels of infections. Moreover, this issue is not mentioned in the literature concerning its influence on power systems. Solving this issue is crucial for ensuring the normal operation of power systems. If a pandemic affects to an elevated number of workers needed to operate a plant, it will not be able to function. Management of the personnel who operate plants during a pandemic is very limited, and complex, because these personnel are highly specialized workers and difficult to replace.

Regarding the risk areas in which the power plants can be located, some works studied this challenge, but from a different point of view to the effects of a pandemic. These works attend terrorist attacks, which also could produce personnel casualties, and they receive more attention in the literature because these attacks occur more often than a global pandemic. One of these works is [10] where new analytical techniques to help mitigate the disruptions to power systems caused by terrorist attacks are presented. Mathematical models have two levels and they allow identifying critical system components with low computational effort. In Ref. [11] authors also present a bi-level model that minimizes the number of components that could be damaged in case of an attack. In recent years, authors of [12] present a review of cyber-attacks on power systems considering a system theoretical perspective.

In order to solve the mentioned issues, a mathematical model that addresses different requirements simultaneously is required. Scheduling of generation and dispatch of electricity, the risk areas due to cases of COVID-19, the availability of personnel that can be diminished by cases of contagion, and the production cost are aspects hard to analyze holistically. To achieve these goals, multi objective optimization is a powerful tool [13] in the energy field [14]. Each value of one objective function is connected to the best from the other objectives. Moreover, the solution to the overall problem is composed of a combination of the optimal solutions for each objective [15]. The study of power generation and economic dispatch by using this methodology has been presented in several approaches. The approach presented in Ref. [16] was one of the first to present a model that addresses jointly the Unit Commitment problem with emissions as a different objective function. The problem is solved by using a weighting method to formulate the bi-objective problem as an optimization model of single-objective. In Ref. [17], a stochastic multi-objective method that considers generating cost, NOx, and the risk due to the variance of active and reactive power mismatch is solved. The test case is an IEEE 11-bus system. Authors of [18] present a multi-objective method that addresses the total cost and emissions as objective functions by using a lexicographic-augmented ε-constraint technique. The approach attends the hydrothermal generation. In Ref. [19], authors present a work to implement an ε-constraint method for obtaining efficient solutions. They propose a variation of the method (called augmented ε-constraint method) that reaches only efficient solutions and avoids redundant iterations by accelerating the whole process. In addition, the method is programmed in the software GAMS by solving problems of the energy sector. Regarding the ε-constrained method, a hybrid method to solve multi-objective problem is developed in Ref. [20]. The proposal combines the ε-constrained method and the Cuckoo method. Authors affirm that the benefit of the method is the high precision and the distribution of its Pareto frontier. Table 1 compares the main characteristics of the aforementioned works. Also, the present paper is also included.

In this context, this paper proposes how to mitigate the effects of COVID-19 in the operation of electric power systems. The goal to ensure the functioning of the systems under different scenarios that may arise due to the pandemic. Studying how the electricity system responds to these changes will make it possible to offer well-founded opinions and develop corrective actions. As a consequence, this paper develops a mathematical approach that presents the following contributions:

- A new method that studies the impact of a pandemic, in this case, the one caused by COVID-19, on the operation of a large-scale electrical system. Differentiating the new proposal from the rest ones that study the variation of demands in these systems. It studies how the pandemic affects different power

Table 1
Comparison between works regarding this proposal.

Domain	[3]	[4]	[5]	[6]	[7]	[8]	[10]	[11]	[12]	[16]	[17]	[18]	[19]	[20]	This work
Pandemic	−	−	−	−	−	+	−	−	−	−	−	−	−	−	+
Personnel casualties	−	−	−	−	−	−	+	+	+	−	−	−	−	−	+
Impact of power demand changes	+	+	+	+	+	−	−	−	−	−	−	−	+	−	+
Terrorist attack	−	−	−	−	−	−	+	+	+	−	−	−	−	−	−
Multi-objetive	−	−	−	−	−	−	−	−	−	+	+	+	+	+	+
Constraints related to worker shifts	−	−	−	−	−	N/D	−	−	−	−	−	−	−	+/−	+

N/D not description found.
+feature included.
+/− feature to be included.
- feature not included.

- This proposal goes beyond of a simple mathematical model that minimizes the power generation or operating costs. It integrates the issues and contributions for more than one entity in charge of the electric power system. In fact, the new proposal handles information regarding to the independent operator of the electric system and health care entities in a holistic manner.
- The proposal considers items that are not taken into account in the literature: the affectation of staff due to cases of contagion. Consequently, the relationship between the reduction of personnel due to infections and generation in the power plants is studied.
- The proposal reduces the gap between the study of social constraints (workers), sanitary measures, and the impacts on energy production and consumption.

plants, depending on the number of cases in different regions and the impact of user behaviors. It relates to the operation of power plants with the availability of workers.
- A multi-objective formulation is performed. The classical multi-objective methods that address the electric power systems only consider as objectives the operation costs and the emissions. The effects of a pandemic have never been considered as one of them. Also, the lexicographic optimization is implemented due to the benefits of this technique.

To prove the efficiency of the proposed model, two systems are studied. First, a 6 bus and 3 generator test system. And second, a real large-scale test case, the Argentine Electric System. With real data about COVID-19 cases.

The remainder of this paper is organized as follows: Section 2 presents and describes the two single-objective models. By contrast, the multi-objective model is detailed in section 3. Section 4 verifies the proposal by solving the two test systems. Results are discussed in Section 5. And the main conclusions are drawn in Section 6. Besides, secondary information is included in the Appendix.

2. Single-objective models

This section describes the two problems that will be solved simultaneously in the following sections. The first model is the widely spread problem of minimizing the generation cost. In addition, the second model is the novel development of this proposal.

2.1. Generating cost model

The first single-objective function (f_1) implicates minimizing the total generating cost. T is the programming horizon, which is set to 24 h. Besides, t is the set of the time period, in this paper is 1 h. The first single objective function is formed by the sum of the variables that represent the power output when each source is considered: thermal units that work with natural gas ($p^g_{i,t}$), thermal units that work with other fossil fuels ($p^{ng}_{i,t}$), hydropower plants ($p^h_{i,t}$), photovoltaic (PV) units ($p^{pv}_{i,t}$), nuclear power plants ($p^n_{i,t}$), wind generators ($p^w_{i,t}$), and the rest of renewables (with lower widespread, $p^r_{i,t}$). Each power output is affected by the generation costs belonging to each source (δ). Regarding generating units, i is the set that corresponds to the generators, and I is the total amount of generators, ϑ_t is the cost of not covered demand, and ncl_t is the not covered demand variable. The second term of (1) is annexed due to the possibility that the total demand cannot be covered. This situation is particularly increased by the existence of the pandemic. The complex condition could lead that there are some power plants unavailable due to the lack of workers.

$$\min f_1 = \sum_{t=1}^{T}\sum_{i=1}^{I}\left(p^g_{i,t}\delta^g + p^{ng}_{i,t}\delta^{ng} + p^h_{i,t}\delta^h + p^n_{i,t}\delta^n + p^w_{i,t}\delta^w + p^{pv}_{i,t}\delta^{pv} + p^r_{i,t}\delta^r\right) + \sum_{t=1}^{T}\vartheta_t\, ncl_t \tag{1}$$

The demand constraint (2) establishes that the sum of all power output must satisfy the total demand. It is formed of the sum of all loads ($ld_{c,t}$).

$$\sum_{c=1}^{C} ld_{c,t} \le \sum_{i=1}^{I} p_{i,t} + ncl_t, \quad t = 1,\ldots,T \tag{2}$$

The spinning reserve (3) is the power available but uncharged that can respond within a few minutes for recompensing eventual issues in the generation. In this paper, the spinning reserve (R_t) is assumed as 10% of total demand. $p^{max}_{i,t}$ is the upper bound of the unit.

$$R_t \le \sum_{i=1}^{I} p^{max}_{i,t} - \sum_{i=1}^{I} p_{i,t}, \quad t = 1,\ldots,T \tag{3}$$

Each unit has a power output limits. They are represented in (4). $p^{min}_{i,t}$ is the lower bound of the generator.

$$p^{min}_{i,t} \le p_{i,t} \le p^{max}_{i,t}, \quad t = 1,\ldots,T;\ \mathrm{i} = 1;\ \mathrm{I} \tag{4}$$

Thermal generation also considers other constraints as startup cost, shutdown cost, up and down ramp operating, hot and cold start cost, maximum, and minimum online time, maximum, and minimum offline time. These constraints are detailed in Ref. [21].

For the hydro generation, the operation curves of these plants are based on relationships between variables for power output, water discharge, and hydraulic head [22]. The representation of power output for hydropower plants is non-linear [23], but it can be represented by using a Mixed Integer Linear Programming (MILP) with a sufficient level of accuracy and reductions of computational effort [24]. Hydropower output is presented by using a MILP model

in Ref. [25].

When PV generation studied, perturbations regarding environmental factors as clouds, thermal effects, or obstacles must be considered. However, PV parks are generally placed in areas with an elevated amount of sunny and clear days in order to increase the efficiency of the collected radiation. The representation of PV generation by considering a deterministic approach is shown in (5). The formula states that PV generation is calculated as the upper bound ($p_i^{pv\_max}$) affected by the PV matrix($\gamma_{i,t}^{pv}$) which contains solar coefficients fluctuating from 0 (without solar radiance) to 1 (maximum solar radiance).

$$p_{i,t}^{pv} \le \gamma_{i,t}^{pv}\, p_i^{pv\_max} \quad , \; i = 1, \ldots, I; t = 1, \ldots, T \tag{5}$$

When the large scale system scheduling is considered, the entity in charge of the operation (generally, Independent System Operator or ISO) programs the pre-dispatch of wind generation several hours before. It is based on wind forecasts and is corrected online. Power generation is represented in (6) and $\gamma_{i,t}^{w}$ is the pre-dispatched generation matrix.

$$p_{i,t}^{w} \le \gamma_{i,t}^{w} \quad , \quad i = 1, \ldots, I; t = 1, \ldots, T. \tag{6}$$

As regards nuclear generation, there are several kinds of nuclear reactors used to produce electricity based on their design [26]. When the nuclear source is an important share of the energy matrix, it is essential to improve the load following capacity. PWR reactors are very widespread at a global level and they can regulate their range up to 5% of the nominal output per minute [27]. As a result, nuclear plants operate three modes (depending on their type): base-load mode (modeled in (7), where Pr_i^n is the rated power for a nuclear generator), frequency control mode [28], and load following. The rest of the operating models are fully described in Ref. [29].

$$p_{i,t}^{n} = Pr_i^{n} \quad , \; i = 1, \ldots, I; t = 1, \ldots, T. \tag{7}$$

In order to model the power transmission, the DC power flow model is adopted ([30]). The power flow variable ($p_{ll,t}$) is represented in (8) as the difference between bus voltage angles ($\theta_{b_i,t} - \theta_{b_o,t}$) divided by the line reactance (x_l).

$$p\_l_{l,t} = \frac{\theta_{b_i,t} - \theta_{b_o,t}}{x_l}, \quad t = 1, \ldots, T \tag{8}$$

The constraint of power balance (9) determines that the sum of power generation, which is transmitted through lines, must cover the demand. The variable $p\_l_{l,b_i,t}$ indicates the power flow entering the bus and $p\_l_{l,b_o,t}$ represents the power flow leaving the bus.

$$\sum_{i=1}^{I} p_{i,t} + \sum_{l=1}^{L} p\_l_{l,b_i,t} - \sum_{l=1}^{L} p\_l_{l,b_o,t} \ge \sum_{c=1}^{C} ld_{c,t} \quad t = 1, \ldots, T \tag{9}$$

2.2. Model for minimizing risk

In this section, the system response to an extreme situation is studied. For this purpose, the response is based on producing the minimum of electricity in dangerous zones, to keep the normal operation. It is remarkable to know how much is the minimum power that can be generated by a portion of the system, which is affected by the COVID-19 pandemic. Several reasons that endanger generation in affected areas:

- The personnel required to operate the plants is not enough due to contagion.
- Liquid or solid fuels for generations cannot be distributed due to restrictions in the transport routes.
- The supply of natural gas can be affected by the pandemic.

To address the personnel planning, the model minimizes the single objective function (f_2), which is expreseed in (10). This represents the generation of the system sectors that belong to zone($i \in RZ$), which is the risk zone.

$$\min f_2 = \sum_{t}^{T} \sum_{i \in RZ=1}^{I} \left(p_{i,t}^{g} + p_{i,t}^{ng} + p_{i,t}^{n} + p_{i,t}^{w} + p_{i,t}^{pv} + p_{i,t}^{r} \right) \tag{10}$$

The generation of each plant belonging to the risk zone is subject to the amount of personnel available to operate it. Where $w_{i,t}$ is the amount of personnel required to operate a generator and pw_i is the amount of MW that can be produced with each available worker.

$$p_{i,t} \le w_{i,t} pw_i, \; \forall \; i \; \varepsilon \; RZ, \; t = 1, \ldots, T \tag{11}$$

In addition, the amount of required workers is limited by upper ($\overline{w_i}$) and lower bounds ($\underline{w_i}$).

$$\underline{w_i} \le w_{i,t} \le \overline{w_i}, \; \forall \; i \; \varepsilon \; RZ, \; t = 1, \ldots, T \tag{12}$$

Initial work status (TW^{ini}) is the number of hours during the employees that operate the unit have been working (if it is positive) or resting (if it is negative) before the first hour of the programming horizon. And, the minimum work or rest (TW_i or TR_i) time is the number of hours in which employees must remain working or rest. Thus, initial work status and minimum work/rest times determine the online (13) or off status (14) of the generator i at the beginning of the programming horizon.

$$p_{i,t} = 0, \quad \forall i \; : TW_i^{ini} < 0; \quad t = 1, \ldots. \left(TR_i + TW^{ini} \right) \tag{13}$$

$$p_{i,t} \ge 0 \quad \forall i \; : TW_i^{ini} > 0; \quad t = 1, \ldots. \left(TW_i - TW^{ini} \right) \tag{14}$$

The number of hours that generator i must remain in online or offline status after initiating the work shift or the work rest is imposed by equations 15–18. When the generator i is online, the value of the binary variable $z_{i,t} = 1$. By contrast, when the generator i is offline, the value of $z_{i,t} = 0$. Besides, T_i^{ini} indicates the number of hours that the generator has been working (if it is positive) or in off status (if it is negative).

$$z_{i,t} - z_{i,t-1} \le z_{i,t+j} \; , \; i = 1, \ldots\ldots I, \; t = 2, \ldots\ldots T, \; j = 1, \ldots\ldots (TW_i - 1) \tag{15}$$

$$z_{i,1} \le z_{i,1+j} \; ; \; \forall i \; : T_i^{ini} < 0; \quad j = 1, \ldots. \; (TW_i - 1) \tag{16}$$

$$z_{i,t+j} \le z_{i,t} - z_{i,t-1} + 1; \; i = 1, \ldots\ldots I, \; t = 2, \ldots\ldots T; j = 1, \ldots\ldots (TR_i - 1) \tag{17}$$

$$z_{i,1+j} \le z_{i,1}; \; \forall i \; : T_i^{ini} > 0, \; j = 1, \ldots\ldots (TR_i - 1) \tag{18}$$

In this context, equations 19 and 20 relate the power output variable $p_{i,t}$ with the binary variable $z_{i,t}$. As a consequence, both equations relate the operation of the generator with the availability of workers and constitute one of the main contributions of this

proposal. The rest of the model includes constraints (2–9), with similar reasoning to the previous subsection, along with the constraints of each generation source.

$$p_{i,t} \leq M(z_{i,t}); \quad i = 1, \ldots, I;\ t = 1, \ldots, T \tag{19}$$

$$p_{i,t} \leq -M(1 - z_{i,t}); \quad i = 1, \ldots, I;\ t = 1, \ldots, T \tag{20}$$

3. Multi-objective optimization

Consider the following multi-objective mathematical model (MMM), where x is a decision of the variable vector ($g(x)$), q is the set of objective functions, $f(x)$ a single objective function, and FR is the feasible region.

$$\min f\left(x\right) = \left[f_1(x), f_2(x), \ldots, f_q(x)\right)\Big] \tag{21}$$

$$s.t\ g(x) \leq 0, \quad x \in FR \tag{22}$$

3.1. Multi-objective model definitions

When multi-objective problems are taken into account, the classical optimality concept is replaced by the Pareto optimality concept [31]. When this concept is considering, a solution cannot be enhanced except if it gets worse the performance in at least one of the rest of objective functions. The vast majority of the methods can be classified as aggregative and non-aggregative methods. Within the former classification, methods can also be divided in the called based on preference and generating ones. The first class includes as the main spread kind is the goal method, which gives preference to a particular objective from the rest ones and presents different priorities. However, the methods are often no preferred because its assessment may, therefore, be affected by subjectivity bias on the part of the operators in charge of solving these problems. Generating methods include the epsilon-constraint (ε—constraint [32])and weighting MMMs. The ε-constraint method is conformed by one main objective function subject to the rest of the objective functions. From the comparison between the two generating methods can be deduced that the main drawback of the weighting methods is having a single objective that is obtained from the multi-objective problem by unifying all objective functions using weighted coefficients [18]. In this regards, the authors of [33,34] compared the two methods and concluded the following differences:

- When linear problems are considering, ε-constraint methods can generate solutions into the entire Pareto frontier. However, the weighting method produces only efficient solutions at extremes.
- The ε -constraint methods can obtain unsupported efficient solutions when multi-objective integer/mixed integer programming models are considered.
- The scaling of the objective functions is not required in the ε-constraint methods, but it is necessary when the weighting methods are considered.
- The amount of efficient solutions is controlled by controlling the number of grid points in each range of objective functions.

Besides, the non-aggregative methods find the whole Pareto front without any need of pre-evaluating the different objective function. Once the whole Pareto front is obtained, different criteria can be applied to select the final solution [35].

Considering the aforementioned statements, the ε-constraint method is chosen to solve the problem of the present paper. A complete description of the method can be found in Ref. [34]. The best values are easily attainable by considering the optimal of the single-optimization. Formulation of the ε-constraint method is presented, in a general manner, as follows (based on [36], where ε is a epsilon value):

$$\begin{aligned} &\min f(x) = f_1(x) \\ &s.t \\ &f_2(x) \geq \varepsilon_2 \\ &\ldots \\ &f_q(x) \geq \varepsilon_q \\ &x \in FR \end{aligned} \tag{23}$$

In the field of ε-constraint methods, the lexicographic optimization is implemented [37]. It constitutes a sequence of objective functions that optimize the first objective function, after, the second objective function, and so on (if there are more objective functions). The lexicographic optimization can be resumed as follows (for a generic case with p single-objective functions):

- The first objective function (main objective) is optimized and z_1^* is obtained.
- The second objective function is optimized while the constraint $f_1 = z_1^*$ is included into the formulation and z_2^*. It helps to determine the value of ε_2.
- If there is a third single-objective function, it will be optimized, and constraint $f_1 = z_1^*$ along with $f_2 = z_2^*$ are considered.
- The processes are repeated until all p objective functions are optimized. It helps to determine the value of ε_q.

The basic formulation of the ε-constraint method by using lexicographic optimization is present as follows (based on [34]). *eps* is sufficient small positive number and r_p is the range of the function number p. Following the same reasoning of the (23) a generic formulation for p single-objective functions is presented. Fig. 1 shows the flowchart that indicates the procedure implement to solve multi-objective problems.

$$\begin{aligned} &\min f(x) = f_1(x) + eps(s_2/r_2 + \ldots + s_q/r_q) \\ &s.t. \\ &f_2(x) - s_2 = \varepsilon_2 \\ &\ldots \\ &f_q(x) - s_q = \varepsilon_q \\ &x \in FR,\ x \in R^+ \end{aligned} \tag{24}$$

For the proposed paper, the multi-objective model is composed of two single-objective functions. Based on the previous nomenclature, the first objective function f_1 is the one described in formula (1) in Section 2.1, the generating cost. The second single-objective function f_2 is the minimization of the generation of risk zones, which was detailed by formula (10) in Section 2.2. The selection of f_1 and f_2 were performed to keep the nature of the unit commitment problems, which are much extended in the literature [29]. Also, as was commented before, one of the advantages of the ε-constraint method is not including in the resolution subjective valuations. This ensures that all solutions are explored objectively.

3.2. Main differences with the classic approaches

Since the model is an optimization one, the reader should not assume that the new model only finds a solution that meets the demand, at the minimum generation cost. The new multi-objective

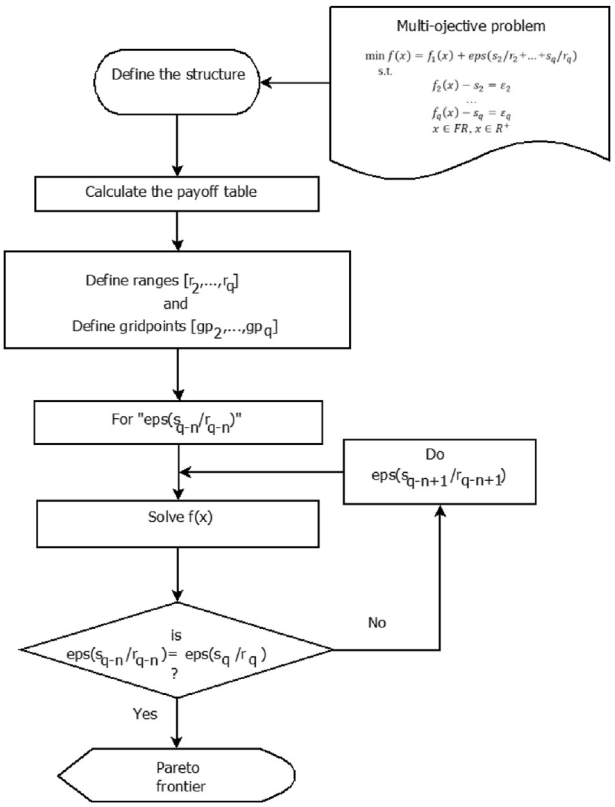

Fig. 1. Flowchart of the procedure to solve multi-objective problems.

formulation goes beyond a mere reduction of the operating costs. As can be observed in the previous section, the new proposal considers the protection of workers in front of the disease, as much important as the efficiency of the system. Some constraints regarding the number of workers who are available to operate the power plants are included in the model.

When all approaches are compared, it can be observed that this approach introduces information about the personnel and how they can be affected by the disease. For instance, the number of generators of a power plant is affected by the concurrence of the workers. It means that if a generator is cheaper but the number of workers to operate it is not enough, the unit cannot be operated and the demand must be covered by more expensive generators. The inclusion of constraints that model these situations is more realistic and appropriate than only computing the mentioned generator as “unavailable”. Within this approach, the utilization of generators can be related to the shift plan of the workers, as can be observed in formulas (15-18). For example, if the available workers only cover one shift, the generators of this plant will be scheduled for covering the power demand during the hours that these workers are available. In a first instance, it could be affirmed that the influence of shift plans can be replaced by the mere definition of the hours that the generator can be operated. However, this affirmation is not scalable for a large system. Consequently, the test cases, where the novel approach must be implemented, are related to the operation of the energy systems of countries, whit thousands of lines and generators. In these situations, the definition of the available hours of the generators without considering the situation of workers is no longer applicable.

Furthermore, it is expected that different entities enter the required data to give a more efficient response to the disease. For example, on the one hand, data related to the electric system can be entered by the Independent System Operator (ISO). On the other hand, the data related to the COVID-19 positive cases and the available workers can be updated by entities in charge of health care. In front of this joint effort, the new proposal finds a better application than the classical approaches, because of the integration of data from different sources. Indeed, the ISO cannot handle the information about COVID-19 positive cases of the workers, and the health entities cannot handle information about the electric systems. As will be discussed in the next sections, the new multi-objective model considers information from both sources.

Another benefit of applying the novel approach is the consideration of the risk zones and contagious reductions. Due to the inclusion of the objective function (10), the model considers zones where cases of COVID-19 are important. This contribution offers two main consequences, the first one is the reduction of the generation in regions where the disease is extended, and the correct operation of the power plants could be unexpectedly interrupted (due to positive cases). The main premise consists of lower operation in dangerous zones, along with lower possibilities that the activities were interrupted due to losses of workers. The second consequence is the reduction of transmission of the disease because a higher number of workers of risk zones remain in their homes. It means that the level of disease transmission is reduced.

3.3. Main considerations about personnel management in this approach

One of the main contributions of this paper is the degree of closeness between the operation of the systems and the effects of pandemic on the employers. Due to the multi-objective mathematical model, the electric system can be operated as efficiently as possible considering the availability of employees. In normal situations, employee availability should not be a major problem, because companies have sufficient staff to cover possible eventualities. But in special situations, such as the COVID-19 pandemic, the situation is much more complex. A large number of employees may be in immediate isolation. For example, if an employee on a shift tests positive for COVID-19, that employee and all employees who have been in direct contact with that employee must be isolated. As a result, in the worst-case scenario, all employees on a shift may be unable to continue working for at least 15 days. In consequence, several strategies can be implemented in the industry for controlling the COVID-19 pandemic [38,39]:

- It is recommended to provide more space between workers (minimum distance of 2 m).
- Allowing, to the extent possible, home office, flexible hours or rotating shifts to reduce the number of work into close contact with each other.
- Avoid all non-essential travel along with meetings and replace them with virtual meetings.
- Workers who belong to high-risk categories due to their age or pre-existing medical conditions must be overprotected or temporally replaced.
- When a suspected COVID-19 case is identified in the power plant, medical advice is required and the worked must be sent home immediately. In addition, the individual should isolate from other workers. Then, all touched items must be disinfected and all persons with whom the suspected infected person may have come into contact should be identified and notified.
- Plant managers should have a plan for handling the situation of workers that develop symptoms in the workplace or before they arrive at the workplace.

- All visitors to plants should be asked about their recent travel history and whether they are currently experiencing any symptoms.
- Names of all persons that visit the power plants, including a record of visited areas.

The basic idea of this model is to reduce the generation of risk areas by offering more flexibility to operate the power systems. The following example better explains the idea. The plant in Fig. 2 has 4 generators with an individual capacity of 25 MW. Each generator requires 3 workers for its operation. The figure shows 3 possible scenarios for the operation of these plants. In case A), each of the 4 generators is operating at maximum capacity, and the total generation is 100 MW. In this case, 16 employees are required in the plant: 12 for the operation of 4 generators and 4 for the rest of the tasks. In case B), 2 generators are working at maximum capacity, while the other two are offline. Because of this, there are only 6 workers attending to the two generators that are in service, and 3 employees performing the rest of the tasks. In case C, all generators are out of service, so the plant does not produce electricity. As a consequence, no employees are required to operate the generators and only 2 employees are needed to perform basic activities to maintain the plant. It is important to clarify that they are ideal cases. There are regulations about the minimum personnel of a power plant, which vary according to the country, and they are not considered in this example because it is only presented as a didactic case.

During a pandemic, the plant personnel may not be able to operate the plant. Or there may be some variants, such as a preference for reducing the number of workers simultaneously in the plant, to increase social distance, and have a greater reserve of personnel at home. This is helpful in case of contagion. If a worker is diagnosed with COVID-19 (called case 1), the chance of infecting other workers is high due to the speed of contagion of the disease [40]. In consequence, an important quantity of the workers could be diagnosed with COVID-19 due to close contact. In light of this situation, health measures can require the effective isolation of many workers or even all workers that were in the plant during the same shift of case 1. For this reason, it is important to keep an adequate reserve of workers.

It is important to mention some considerations about the application of the proposed model. Regarding the hourly shift changes, they can be considered on an individual basis (the hours that each employee can remain working are analyzed). Equations 11 and 12 show that each of the generators depends on a minimum number of employees to operate. A shift change directly affects the operation of the generators, if there is a variation in the number of employees between one shift and the other. To better understand this, the example in Fig. 2 can be considered again. Assuming that in the shift change, the number of employees changes from case A) to case B). Consequently, two generators will no longer be available (based eq. 11 and 12). If in the opposite case, during the shift change, the number of workers moves from case B) to A), two more generators will be available. However, the proposed model goes beyond a mere analysis of the shift change of employees but analyzes for each period the availability of employees. This can be seen in a more extreme example. Suppose that in the example in Fig. 2 at shift change there is 1 employee less than the minimum number needed to operate the 4 generators in scenario A. In this case, only 3 of the 4 generators can be operated (assuming that no reserve employees can be obtained).

Regarding the organization of the logistics of these employees, the model assumes that each company considers the availability of its employees, including the logistics necessary for these employees to be able to go to the workplace in case they are needed. To better understand the scope it is convenient to explain it with a real case from Argentina. In the province of Santa Fe, is located the thermoelectric plant Brigadier López [41], this plant has employees who live in that province, and also employees in the neighboring province of Entre Ríos. Due to the pandemic, the managers of this plant decided to count as available only employees residing in the province of Santa Fe, and not those from the province of Entre Ríos. The main reason is to reduce the risk that employees from Entre Ríos might become infected due to the greater distance they have to travel, and to the fact that the only via of connection (the Paraná-Santa Fe Sub fluvial Tunnel, Raúl Uranga-Carlos Sylvestre Begnis)

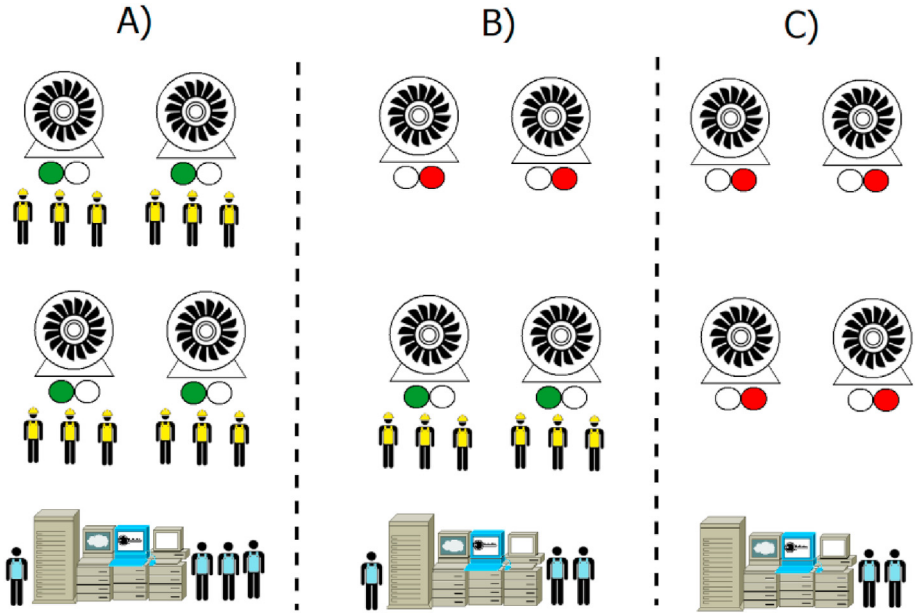

Fig. 2. A. Scheme of a power plant at the maximum operation level. Fig. 2B. Scheme of a power plant at the medium operation level. Fig. 2C. Scheme of a power plant at the low operation level.

had very restricted circulation. For this case, it was preferred that in case the available workers (in Santa Fe) could not cover all the necessary shifts, the production of this plant would be replaced by the generation of others, rather than assuming the risk of transferring the employees from Entre Ríos. The main reason for this consideration is that the model is directed towards the ISO figure, which is a central system where the availability of employees cannot be differentiated, but the availability of each generator can be differentiated. This is why the present work serves as a link between the operation of the electrical system through the ISO, and the reality of each employee of each plant, through the information that the plant managers load into the mathematical model (or send the information to the ISO).

4. Test systems and limitations

In order to demonstrate the effectiveness of the novel proposal, two test systems are studied. The first is a small 6-bus system. And the second one is a real system, the Argentinean Large Scale System. Besides, the Argentine System includes real data about COVID-19 pandemic, to measure better the contribution of this paper.

The models are solved in GAMS [42] by using the solver CPLEX [43] with a relative gap of 0.0005%. The software is a high level modeling system that is extended in the field of optimization and mathematical programming in general. It contains language compiler and a large amount of associated solvers as CPLEX and Gurobi. This software allows researchers to quickly represent complex optimization problems into workstation code. Its architecture offers high flexibility, by permitting shifting the solvers selected without altering the formulation of the original code. The programming horizon is one day with a period of 1 h. The reason to choose this programming horizon is the dynamic of the pandemic. The effects that this disease can produce in the available personal change every day. For this reason, a larger programming horizon would lack practicality in this context. The used PC has an AMD A6-34000 M APU processor along with a Radeon HD Graphics @ 1.40 Ghz. The RAM memory is 8 GB.

In connection with the limits of this work, the procedure for solving the multi-objective models adopted by this paper is fully described in Refs. [19,20]. The data for generating units and transmission lines is presented in Refs. [44,45] for both systems. Also, the particular limits of each system are detailed in the corresponding subsection. Besides, for the Argentine System, it is assumed that the online generators have enough spinning reserve available under the great number of generators in the system. Regarding nuclear generation, only the base-load mode is considered for the units. This is the most efficient mode, but it is unable to meet peaks of consumption.

For worker consideration, it is assumed that the plants can be operated 24 h a day, in three shifts of 8 h each. It is assumed that employees go to the plant to work during their shift and return home at the end of their shift. No other alternatives were considered because in the main case study (the Argentinean system), all plant managers have agreed to maintain the traditional 3-shift type of work. Other types of work forms would not be representative of the main case study. However, extra measures have been taken due to the pandemic, such as not considering employees who are far away from the plant as available. As explained before.

4.1. 6-bus test system

This small-scale problem is composed of 6 buses along with 3 generators and 11 lines. Information about this system can be found on [44]. However, the limits of the lines were changed to better observe the operation of the model by considering different lines. New capacities are: 80, 100, 60, 15, 60, 10, 30, 20, 50, 15 and 10 MW from line 1 to 11, respectively. The one-line diagram of the system is shown in Fig. 3. It will be assumed that each generator corresponds to a power plant. In consequence, the system also has three power plants.

Two cases are considered for the system. The first one is the normal operation without considering the pandemic. This case assumes that all workers are available to operate the three generators for 24 h at their maximum capacity. This means that the value of.

$\overline{w_i}$ is obtained by dividing the maximum capacity of each generator (expressed in Ref. [44]) by the value of pw_i (for this scenario is 0.483 *workers*/*MWh*). The model that represents the situation is the one presented in section 2.1. It is composed of 2396 equations, 961 single variables, and 72 binary variables. The total cost is USD 77,775 and the CPU time is 0.63 s. Based on the obtained results, the numbers of minimum workers required in each plant are the following. For plant 1 (G1), the values of w_1 457, 486, and 474 workers. It is important to mention that three values of w_1 are presented because it will be assumed that there are three shifts (between hours 1–8, 8–17, and 17–24). For the second plant, the values of w_2 for each shift are 0, 42, and 48 workers. Besides, values for w_3 are 0, 0, and 91 workers. It is important to mention that values of w_i are obtained from theoretical information. They are not related to a real case because the 6-bus test system does not include in the original study in Ref. [44] the influence of the worker availability.

The second case also considers the presence of the pandemic in the zone of the power plant that operates the generator G2. By contrast, zones of G1 and G3 are not affected by COVID-19 cases and they have full availability of workers. As a result, equations 10–20 are applied to G2, in addition to the previous ones. The model that represents this case handles two objective function and the equations are the ones explained in Sections 2.1 and 2.2. For solving the system using the ε-constraint method, the objective function of f_1 (section 2.1) is kept and the other objective function (f_2) is annexed to the constraints. f_2 is solve twice in order to define the range of ε. Once f_2 is solving by minimizing and one by maximizing. In consequence, the range of the total production of the generator G3 is between 38 and 186 MW. The necessary parameters of this case, including how many employees are distributed by facility types (related to the available personnel), are included in Table A1 in the **Appendix**. The Pareto frontier with the objective values for f_1 and f_2 is shown in Fig. 4. The method generates 400 iterations and each model, which is formulated by following (22), is composed of

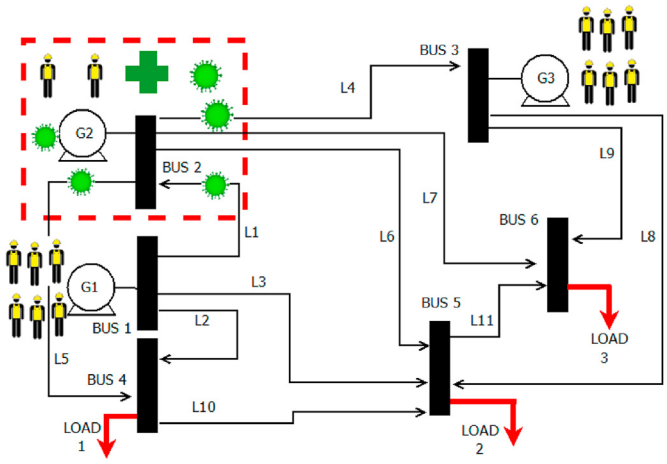

Fig. 3. 3 bus system one-line diagram. Zone of generator 2 is affected by the pandemic.

4056 single equations, 1033 single variables, and 144 binary variables. The 400 iterations are solved within a CPU time of 4 min. The values of w_i for the three shifts fluctuate depending on the selected solution. The lower generation in each plant, the lower the number of required workers. For instance, a solution that implies the minimum possible value of total generation of G2, 38 MWh during the whole programming horizon, presents the following values of w_i. For plant 1: 457, 486, and 475 workers. For plant 2: 0 workers during the whole day. Besides, plant 3 requires 0, 62, and 91 workers for each shift.

4.2. Argentine electric test system

The main generation technology of the Argentine Electric System (SADI) is the thermal one, as a consequence of the natural gas availability. In addition, there is an important share of hydro generation. The SADI is composed of nine regions. Data belonging to installed power and demand of SADI can be found in Refs. [25,46]. Besides, data regarding the generating costs can be found in Ref. [29]. There are some considerations for the system. Over 50% of the total power consumption belongs to the regions BAS-GBA. Each region is provided by only one Distribution Company (regulated monopoly). Based on [47,48], the energy matrix of the country is composed of thermal source 61%, hydro 27%, other renewables 8%, and nuclear 4%. In addition, data of the demand for the considered day (August 13, 2020) can be found in Ref. [49], and information on the main system lines is included in Ref. [3]. The electric system scheme can be observed in Fig. 5A. In the figure, the main buses (labeled as E1-E15) are marked along with the 500 kV lines, and the nine regions. Information about the power plants located in each region has been included in tables A.3-A.11 in the **Appendix**.

When the system operation is solved without considering the COVID-19 pandemic, by minimizing the single objective function $f_1(x)$, the total generating cost is USD 18,154,497, and the CPU time is 0.8 Sec. The model is composed of 12,361 single equations, 9433 single variables, and 1392 binary variables. The results of this model are discussed in the next section. Moreover, when the scenario also considers the situation with COVID-19 infection cases, the distribution in the country is based on the official report of [50]. On August 13, 2020, there are 268,404 total confirmed cases and 5088 deaths in Argentina. The distribution of active cases in the country can be seen in Fig. 5B. Red circles are drawn in proportion to the number of cases in each province and the data about cases is presented in Table A2, in the Appendix.

Regarding the above, for this case, the objective function of $f_2(x)$ is minimizing the generation of all generators connected to the bus

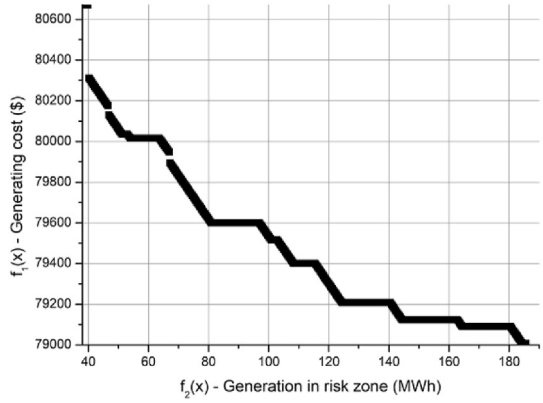

Fig. 4. Pareto frontier of 6 bus system when the zone of generator G2 is affected by the pandemic.

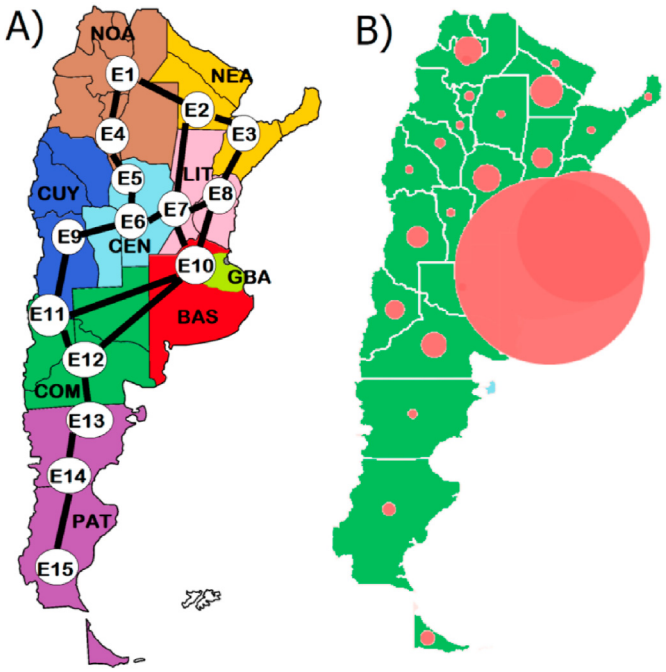

Fig. 5. A. Argentine Electric System one-line diagram. Fig. 5B. Distribution of COVID-19 cases in Argentina.

E10. However, the rest of the constraints are kept. The basic idea is to reduce the generation of units in the bus E10, in order to reduce the required personnel and the risk of infections. The units from the rest of the buses must increase their production to compensate for the decrease of E10 while the total generating cost is reduced. Furthermore, the multi-objective problem is formulating with similar reasoning to the previous case (the objective function of $f_1(x)$ is minimizing the generating cost of the whole system). Data about the personnel in charge of operating the power plants of E10 are not available for the study. In consequence, the generation of E10 is reduced as much as possible while the normal electricity supply is ensured. Besides, to give a better response to the COVID-19 issue, the integration of several entities of Argentina is needed. As consequence, joint work is performed between the Independent System Operator (ISO, which is the CAMMESA Company in the case of Argentina) and the Ministry of Health of Argentina. The ISO provides all information regarding the situation of the electric system. In a similar manner, the Ministry of Health provides information about the COVID-19 cases and the protocols concerning this disease. The integration of both entities is one of the main contributions of the new proposal. This differentiates the proposal from the rest of the classical approaches that handle the problem of minimizing generating costs.

The operative range for (and, in consequence, the payoff table) $f_2(x)$ is between 55,618.5 MWh and 63,000 and the pace is 18.5. The problem is solved in 400 successive iterations in order to obtain accurate solutions and the Pareto frontier is shown in Fig. 6. When the range value is higher than 62,500 MWh, the objective value of $f_1(x)$ is not enhanced. By contrast, when the value of the range is lower than 55,713 MWh the problem is infeasible. In fact, the bus E10 cannot reduce its generation below that level because the transmission lines are working at their maximum capacities. Consequently, more generation from other regions cannot be transmitted to E10. To address this, the generation of a minimum daily amount of 55,713 MWh (considering a certain margin of safety) with the generators of E10 is required for ensuring the

Table 2
Values of daily generation and required workers. Scenario without COVID-19 cases and case with COVID-19 cases.

Region	Without COVID -19 Cases		With COVID -19 Cases	
	Daily generation (MWh)	Workers	Daily generation (MWh)	Workers
BAS-GBA	62123.829	5979	59373.997	4857
CEN	19701.38	1896	19224.681	1573
COM	86053.67	8282	85010.779	6954
CUY	5200.69	501	4415.423	361
LIT	52501.697	5053	54749.327	4479
NEA	74071.023	7128	74379.2	6084
NOA	17126.502	1648	17224.646	1409
PAT	7937.119	764	10337.855	846

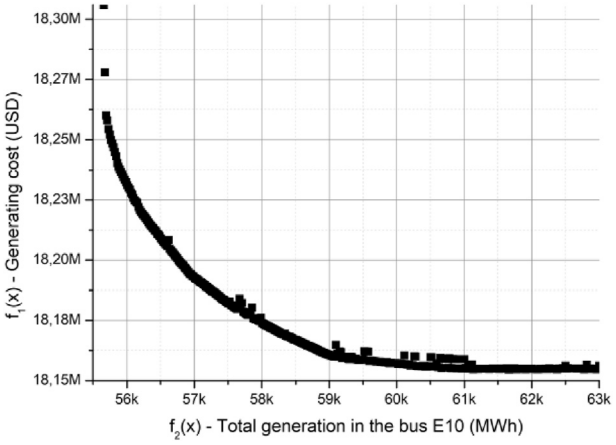

Fig. 6. Pareto frontier of the Argentine Electric System with the E10 region affected by the pandemic.

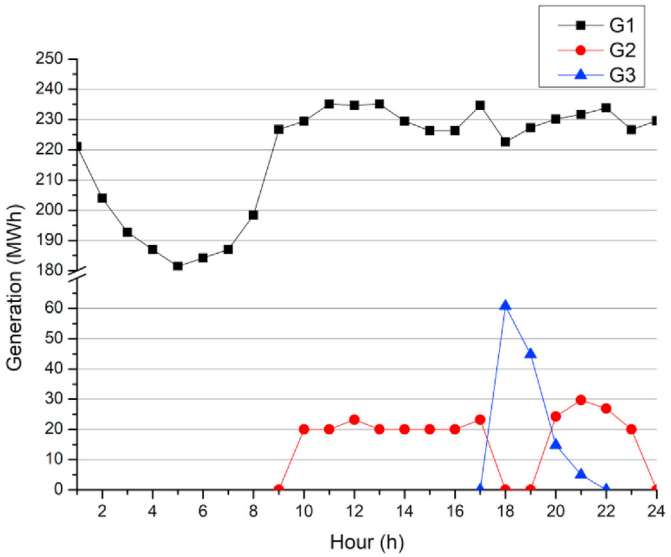

Fig. 7. Generation profile of 6 bus system when the COVID-19 cases are not considered.

normal supply for the regions GBA-BAS. Each model is composed of 12,362 single equations, 9433 single variables, and 1392 binary variables. The total CPU required for solving the 400 iterations is 9 min 20 s.

5. Analysis and discussion of results

The analysis of the results of the two test systems is useful to observe how their operation can be improved. It is a procedure that is helpful to study the impact of changes in an independent variable produces in a dependent variable. It shows the impact that an increase or decrease in the value of a factor concerns the final result in technical analysis. When minimizing power generation cost is considered, it is interesting to know how the changes in the generation of risk zones affect the total cost.

5.1. Results of 6 bus system

Fig. 7 shows the generation profile of the 6-bus system when the effects of COVID-19 cases are not considered. Unit G1 produces the major portion of the generation due to its lower production costs. In fact, the unit generates 5235 MWh at the end of the programming horizon. By contrast, G2 only generates 267.2 MWh and G3 produces 125.3 MWh by virtue of their higher costs.

Nevertheless, when the multi-objective problem due to the pandemic is considered, several feasible solutions are obtained. In this regard, Fig. 8A illustrates the differences between solutions of G1 and G3 production based on the results of 400 iterations. These generators are in charge of replacing the production of G2 when restrictions due to the pandemic are applied. In contrast, Fig. 8B shows the values of the different solutions for the G2 generation. In order to show a more clear idea of the variations, the solutions that are shown in both figures maintain an equidistance of 20 iterations from each other.

It is important to mention that the bounds of required personnel presented in Table A1 are based on reports of [51]. It considers the capacity of power generation of each plant. When the multi-objective optimization method is applied, the total amount of required workers to operate the plant the in risk zone during the whole programming horizon is between 114 and 372 workers. The final amount depends on the selected solution of the Pareto frontier. This constitutes a reduction of the total required personnel between 26% and 16%. The total demand is completely covered for both scenarios of the 6-bus system. This means that the value of the second term of (1) is 0. The availability of workers is enough to cover the total demand. However, if the unavailability of workers is increased, the operation of plants could be reduced. As a consequence, the value of the variable, which represents the not covered demand, will be increased in order to maintain the feasibility of the mathematical problem.

The standard deviation (SD) is a measure implemented to quantify the variation of a numerical amount. Low values of standard deviation indicate that the major portion of the data is closer to their mean (μ). This definition is implemented because the generation values vary during each hour and the difference responds to changes of demands, and it is not caused by the implementation of 400 iterations.

For the case of G1, the total mean (when 24 h are considered) is 219.5 MW, 3.08 MW for G2, and 11.15 MW for G3. By applying

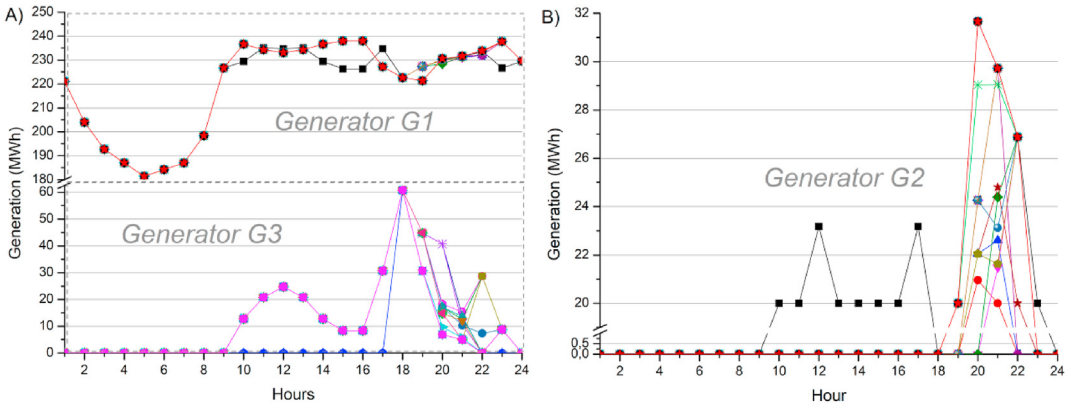

Fig. 8. A. Generation profile of G1 and G3 for different solutions (when the COVID-19 cases are considered). Fig. 8B. Generation profile of G2 for different solutions (when the COVID-19 cases are considered).

similar reasoning, total SDs are 0.67, 2.87, and 2.50 for the three generators, respectively. Fig. 9A shows three hourly means and Fig. 9B illustrates the three hourly SDs. When the values of SDs are analyzed, it can be noted that higher variations correspond to G2 and G3, with a special impact between hours 17–22. Increases in the values of SD are due to the increases in the values of demand, which are produced during the same time interval.

5.2. Results of Argentine Electric System

In connection with the results of the Argentine System (SADI), Fig. 10A shows the results of the accumulated generation/consumption, considering the nine regions and the sources, and Fig. 10B. presents the generation profile by considering the 15 buses. Both figures represent results when the influence of COVID-19 cases is not taken into account. As regards accumulated generation, regions GBA-BAS sum the higher value of consumption (172,456 MWh). NEA region presents the higher value of total generation (74,071 MWh) due to the availability of the hydro generation (it constitutes the 88% of the total generation of NEA region), and in the second place is GBA-BAS regions (generation of 62,124 MWh) with a predominance of natural gas and nuclear sources (44.5 and 42%, respectively). Similarly, the hourly profile per bus indicates that the E12 bus, which corresponds to the COM region, is the bus with a higher value of generation (74,500 MWh). In addition, buses E10 (62,123 MWh), E3 (51,784 MWh), E4 (34,315 MWh) and E2 (22,286 MWh) are next in line in terms of total generation.

Nonetheless, when the 400 iterations for solving the multi-objective problem are considered, the generation of bus E10 (risk zone) is considered, with the presence of COVID-19 cases. Fig. 11 presents the values of different solutions for bus E10. The solutions intervals have equidistance as in the previous section. It is important to remember that as the lower generation of E10 the higher the total cost. Generation of E10 does not have an elevated level of flexibility because the number of lines, which can supply this bus from other regions, is reduced. As can be observed in Fig. 5. A, the bus E10 can directly receive the surplus of buses E7, E8, E11, and E12 through single lines. However, the amount of electricity that E10 can receive is limited by the capacity of these lines. Even more, if the surplus is sending to E10 from a bus different to the previously mentioned, the transmission is limited by the cascade (an arrangement between connected lines) conformed of the lines next to E10 and the other lines.

When the variations of solutions are studied, Fig. 12A illustrates the hourly mean of E10 generation. The values of the range are between 1304 MWh (hour 5) and 4534 (hour 21). Besides, the total mean, which is calculated when the whole programming horizon is considered, is 2469 MWh. Yet, the most important part of the study is determining the degree of variation of the obtained results throughout 400 iterations. This data is shown in Fig. 12. B. In the figure, it can be observed that values of SDs are higher during the hour intervals 1–2 (average of 587 MWh), 9–14 (average of 283 MWh), and 19–23 (average of 254 MWh).

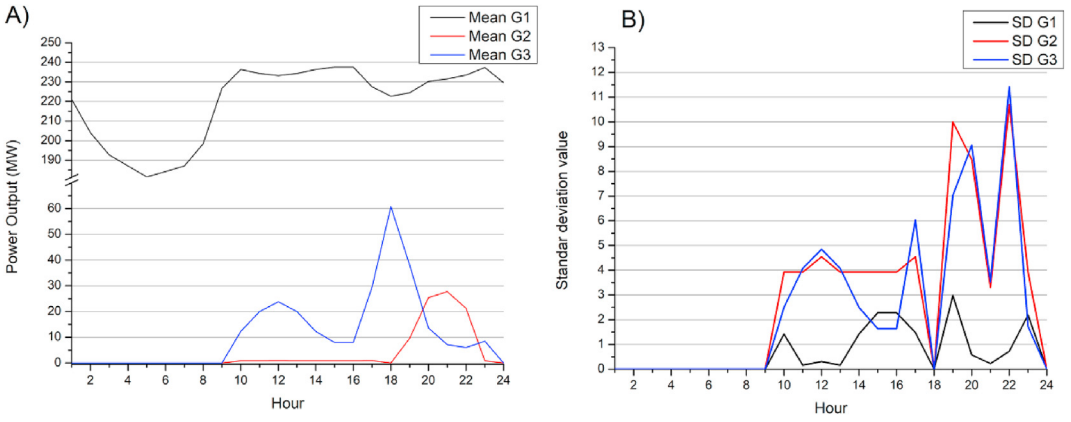

Fig. 9. A. Means of the 6 bus systems. Fig. 9B. Standard deviations of 6 bus systems.

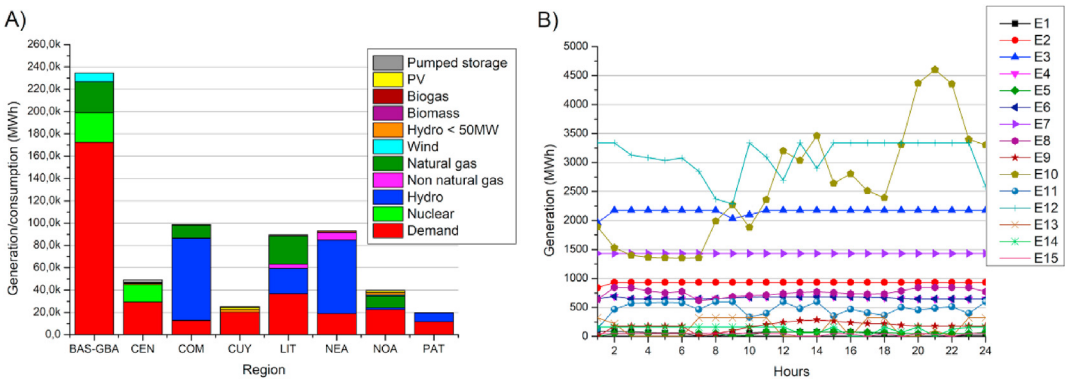

Fig. 10. A. Accumulated generation/consumption profile of Argentine System per region without COVID-19 cases. Fig. 10. B. Generation profile Argentine System per bus without COVID-19 cases.

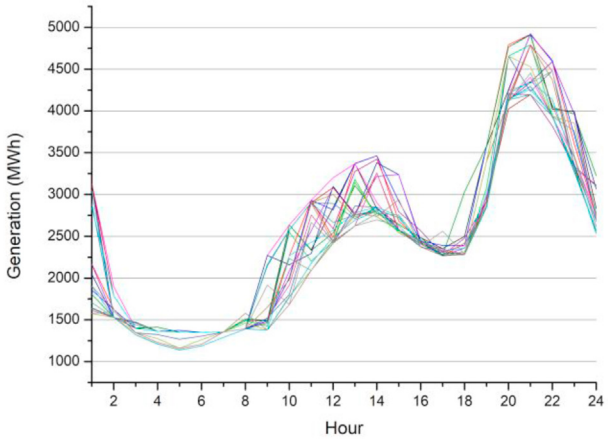

Fig. 11. Generation profile of E10 when 400 iterations due to the COVID-19 cases are considered. Argentine System.

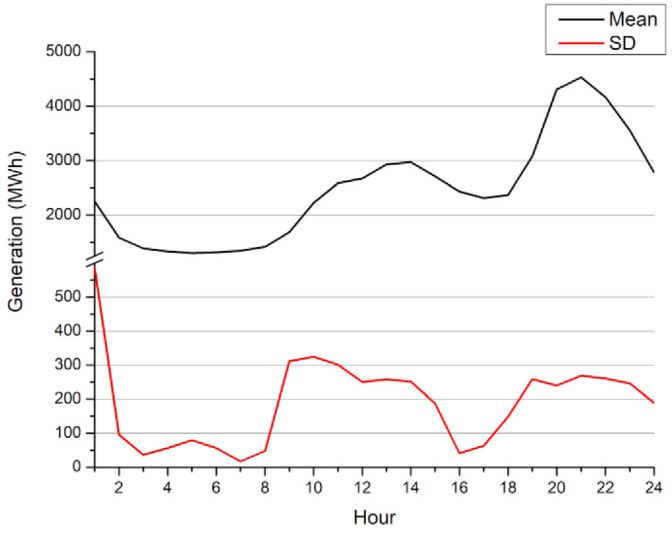

Fig. 12. A. Means of the 6 bus systems. Fig. 12B. Standard deviations of 6 bus systems.

For this scenario, the value of the second term of (1) is also 0. This is due to the total demand is completely covered by the available plants. The availability of workers is enough to operate the required power plants. However, if the unavailability of workers is increased, for example, if the number of positive COVID-19 cases is increased, the operation of plants could be dramatically affected. In this situation, the value of the variable ncl_t, the not covered demand, will be augmented to continue the feasibility of the mathematical problem. Regarding recommendations on shift management. At the moment, considering the results and the recent events of the pandemic, it is still too early to make final assertions on whether it is more convenient the daily shift plans based on hourly consumption profile, or not. Given the observed results, it can be deduced that it would be convenient to reorganize electricity production, considering both shift availability and system efficiency. This is precisely what is obtained with the new multi-objective model proposed in this work.

Regarding the comparison between scenarios, Table 2 presents the values of daily generations when both scenarios are considered (without pandemic and with pandemic). The table detail the generation of each region of the system. The selected solution for the COVID-19 scenario is the one that considers the lowest possible generation of E10. Besides, the table also indicates an estimated number of the required workers (in the whole country for both scenarios). The numbers of workers are estimated based on the report of [52]. Obtaining the number of workers that belong to each plant is not possible due to the confidential character of this information.

Regarding the impact of the pandemic on electricity demand, the ISO in charge of the programming of the Argentine electricity system made a report about this phenomenon. In this study, the ISO evaluates the effects of the pandemic, more precisely of the strict quarantine that took place in the country as of March 20, 2020 [49]. It concludes that in the first months of the quarantine there was a decrease in total demand in the order of 7.9%. Much of the large demand drop for the month of March 2020 (since March 20, 2020) was produced because of the preventive and mandatory social isolation. If the so-called GUMAs (Large Users by its acronym in Spanish, approximately 60 of the large demand) are observed, there is a decrease of 37% in average values of demand concerning what occurred in the days before the establishment of the quarantine. The drop in the industrial branch stands out, with a decrease of around 50%. However, if the total variation of the high demand is analyzed, in general for the month of March 2020, the drop in power demand depends largely on the lower demand in those industries with the highest demand. The drop is largely due to the lower demand in those industries related to metal products,

construction, chemicals, rubber, and similar products.

5.3. Generalization of several factors identified in the results

From the study of results of both test cases (6-bus system and the Argentine system), several generalizations about the conditions and factors can be identified in both cases. Indeed, three main factors can be observed in the analysis of both test cases:

1. Effects of the COVID-19 positive cases: as observed in the test cases, the number of positive cases directly affects the normal operation of the electrical systems. According to the results, the areas with a high danger of contagion (G2 in the case of the 6-bus system and E10 in the case of the Argentine system) are places with high volatility, in terms of system operation. This is because they are places that are prone to an increase in the number of cases, with the potential risk of affecting a significant number of workers. The best way to minimize this impact is to apply the sanitary measures mentioned in Sections 2 and 3.

2. System efficiency reduction: the efficiency of the system is deeply affected by the pandemic. Two main reasons reduce system efficiency. The first one is the number of positive cases, which can mean that a power plant cannot operate due to a lack of workers. The consequence of this is that more expensive generators have to be committed, or the required electricity has to be transported from more remote locations. This increases the cost of production. The second reason is the changes in the demand curve. Insulation measures have caused changes in the electricity demand curve. This is opposite to the design of electric systems. In most countries, the normal curves (without pandemic) respond to a characteristic demand with peaks that, although they may vary between countries, are between hours 11–13 and between hours 20–23. Therefore, strong changes in demand may force systems to operate under conditions different from those for which they were originally designed.

3. Service quality risk: as could be seen in the results (in both systems), critical units are crucial because their generation cannot be fully replaced. In the case of the 6-bus system, the production of G2 could not be fully replaced by G1 and G3. And in the Argentine system, it was observed that the production of bus E10 cannot be fully replaced by the rest (due to demographic reasons). All this means that if there is a very large number of cases of the disease, which does not allow the operation of G2 and E10 (even in a reduced form of operation), probably, many users will not receive the service. Certainly, emergency equipment would be put into operation for essential services, but a large part of the population would not have electricity. All this is due to the rigidity of these power systems, which do not allow much flexibility in the face of unforeseen situations such as a pandemic.

6. Conclusion

This paper presented a new multi-objective mathematical model that is implemented to determine the optimum operation of an electric power system. The novel model is specially developed to attend one of the most complex problems faced by humanity, the COVID-19 pandemic. In particular, this paper deals with the enhancing of the operations of electric systems located in regions where the number of confirmed cases of the disease is high. The main difference between this proposal and other ones, available in the literature, is that it considers the minimization of generation in risk zones as an objective function, besides the classical ones. In this way, the present paper becomes an option to face the diseases and its elevated level of infection. The key benefits of the proposed model are reduction of the generation power in power plants that are located in places where the contagious are considerable but without neglecting the minimization of operative costs. The lower the generation in the risk zone, the more optimist scenarios to develop actions to mitigate the disease, such as the social distancing. It considers the impact of the pandemic on different power plants considering the number of cases in different regions. Besides, constraints for worker shifts are developed to protect the personnel and reduce their exposition to possible contagions.

To test the effectiveness of the model two systems are studied. The first one is the 6-bus system that considers the unit G2 is located in a risk zone. The generation of this unit is replaced by the rest of the generators (G1 and G3). The total cost can be increased by 1.5–3.7% (depending on the maximum amount of generation allowed for G2) along with reductions of the generation in the risk zones up to 80%. The second system is a real case, the Argentinean Electric System. Data implemented is based on reports of official electricity and health entities. These reports indicate the union of regions GBA-BAS represents the more risky area. When all iterations of the method are performed, it can be observed that total cost can be increased by 0.009–0.8% along with generation reductions of up to 12% in the risk zones. The reason for the low range of decrease is that the generation of these regions cannot be largely reduced by limitations regarding transmission lines. By the analysis of results, some factors can be generalized to improve the measures taken to combat this disease.

By the end of this conclusion, it can be noted that the novel proposal presents several contributions to face the pandemic. The robustness of the electric power system is enhanced, in terms of keeping the service, in front of the effects of the disease. The combination of system efficiency and health measures in the proposal is confirmed when the availabilities of generators are committed (by following the medical certificates of the capacity of workers that operate the power plants). Another contribution is the integration between the efforts of Independent System Operators and Health Care Entities. This is one of the keys of the paper and it is often not holistically considered by the literature. As more information will be obtained on the progress of the fighting against the COVID-19, this method will find better applications. The model obtains feasible solutions with a low computational requirement. Also, it can be easily adapted to the systems of other countries.

Declaration of competing interest

The authors declare that they have no known competing financial interests or personal relationships that could have appeared to influence the work reported in this paper.

Acknowledgment

Author would like to thank National Scientific and Technical Research Council (CONICET).

Appendix

Table A.1
Parameters for the 6-bus system.

Parameter	G1	G2	G3
T_i^{ini}	1	−3	1
TW_i	8	8	8
TR_i	16	16	16
$\frac{w_i}{}$	40	40	10
$\overline{w_i}$	520	440	160
pw_i	0.483	0.483	0.483

Table A.2
Accumulated cases of COVID-19 in Argentina at August 13, 2020.

Province	Accumulated cases	Region	Province	Accumulated cases	Region
Buenos Aires	171,381	BAS-GBA	Mendoza	2745	CUY
Buenos Aires City	74,592	BAS-GBA	Misiones	55	NEA
Catamarca	63	NOA	Neuquén	1719	COM
Chaco	4279	NEA	Río Negro	3535	COM
Chubut	384	PAT	Salta	824	NOA
Cordoba	4146	CEN	San Luis	23	CUY
Corrientes	222	NEA	Santa Cruz	33	PAT
Entre Ríos	1365	LIT	Santa Fe	2764	LIT
Formosa	78	NEA	Santiago del Estero	199	NOEA
Jujuy	4203	NOA	Tierra del Fuego	1226	PAT
La Pampa	181	COM	Tucumán	502	NOA
La Rioja	639	CUY			

Table A.3
Power plant information. Buenos Aires Region (BAS-GBA). Based on [53].

Source	Name	Number of units	Capacity (MW)	Unitary Cost (USD/MWh)
THERMAL	AES- PARANA	2	263	25.525
THERMAL	AES- PARANA	1	319	24.125
THERMAL	ARGENER	1	190	27.35
THERMAL	ARRECIFES	20	1	32.075
THERMAL	BAHIA BLANCA	2	310	24.35
THERMAL	BARRAGAN	2	280	25.1
THERMAL	BRAGADO	4	30	31.35
THERMAL	BRAGADO	2	24	31.5
THERMAL	BROWN	22	1.2	32.07
THERMAL	CAPITAN SARMIENTO	6	1	32.075
THERMAL	CERRI	1	14	31.75
THERMAL	CLAROMECO	1	0.75	32.08125
THERMAL	COLON BS AS	19	0.8	32.08
THERMAL	COSTANERA	4	9	31.875
THERMAL	COSTANERA	4	120	29.1
THERMAL	COSTANERA	2	256	25.7
THERMAL	COSTANERA	1	310	24.35
THERMAL	COSTANERA	1	350	23.35
THERMAL	COSTANERA	1	308	24.4
THERMAL	COSTANERA	1	120	29.1
THERMAL	COSTANERA	1	220	26.6
THERMAL	DIQUE	2	17	31.675
THERMAL	DOCK SUD	2	37	31.175
THERMAL	DOCK SUD	1	256	25.7
THERMAL	DOCK SUD	1	256	25.7
THERMAL	DOCK SUD	1	288	24.9
THERMAL	ENSENADA	1	155	28.225
THERMAL	GENELBA	1	219	26.625
THERMAL	GENELBA	1	219	26.625
THERMAL	GENELBA	1	236	26.2
THERMAL	GENELBA	1	181	27.575
THERMAL	GENELBA	1	187	27.425
THERMAL	GENELBA	1	193	27.275
THERMAL	GRAL BELGRANO	3	260	25.6
THERMAL	JUNIN	16	1.4	32.065
THERMAL	LA PLATA	54	0.6	32.085
THERMAL	LA PLATA	10	1.2	32.07
THERMAL	LAS ARMAS	2	5.5	31.9625
THERMAL	LAS ARMAS	1	24	31.5
THERMAL	LINCOLS	13	1	32.075
THERMAL	LOBOS	19	0.84	32.079
THERMAL	MAR DEL PLATA	2	51	30.825
THERMAL	MAR DEL PLATA	2	15	31.725
THERMAL	MAR DEL PLATA	1	25	31.475
THERMAL	MAR DEL PLATA	1	28	31.4
THERMAL	MAR DEL PLATA	1	25	31.475
THERMAL	MAR DEL PLATA	1	28	31.4
THERMAL	MAR DEL PLATA	1	25	31.475
THERMAL	MAR DEL PLATA	1	17	31.675
THERMAL	MIRAMAR	15	1.4	32.065
THERMAL	NECOCHEA	2	33	31.275
THERMAL	NECOCHEA	2	70	30.35

Table A.3 (*continued*)

Source	Name	Number of units	Capacity (MW)	Unitary Cost (USD/MWh)
THERMAL	NECOCHEA	1	38	31.15
THERMAL	NUEVO PUERTO	1	250	25.85
THERMAL	NUEVO PUERTO	1	110	29.35
THERMAL	NUEVO PUERTO	1	60	30.6
THERMAL	OLAVARRIA	2	19	31.625
THERMAL	PINAMAR	1	16	31.7
THERMAL	PINAMAR	1	17	31.675
THERMAL	PUERTO	1	251	25.825
THERMAL	PUERTO	1	251	25.825
THERMAL	PUERTO	1	282	25.05
THERMAL	PUERTO NUEVO	1	145	28.475
THERMAL	PUERTO NUEVO	1	194	27.25
THERMAL	PUERTO NUEVO	1	250	25.85
THERMAL	SALTO	1	60	30.6
THERMAL	SAN MARTIN	5	1.4	32.065
THERMAL	SAN MIGUEL	6	2	32.05
THERMAL	SAN NICOLAS	1	350	23.35
THERMAL	TANDIL	4	50	30.85
THERMAL	VILLA GESELL	1	17	31.675
THERMAL	VILLA GESELL	1	80	30.1
THERMAL	VILLA GESELL	1	16	31.7
THERMAL	VILLA GESELL	1	15	31.725
THERMAL	VILLEGAS	1	23	31.525
WIND	CORTI	29	3.45	31.21375
WIND	CENTENARIO	3	100	28.8
WIND	LA CASTELLANA	32	3.125	31.221875
WIND	VILLALONGA	15	3.4	31.215
NUCLEAR	ATUCHA I	1	370	18.75
NUCLEAR	ATUCHA II	1	745	9.375
SOLAR PV	PUNTA ALTA	2	60	29.8

Table A.4
Power plant information. Patagonia Region (PAT) Region. Based on [53].

Source	Name	Number of units	Capacity (MW)	Unitary Cost (USD/MWh)
THERMAL	A. MANAT BEHR	1	15	30.725
THERMAL	ALUAR	4	31.3	30.3175
THERMAL	ALUAR	2	38.5	30.1375
THERMAL	ALUAR	2	38.6	30.135
THERMAL	ALUAR	2	165	26.975
THERMAL	ALUAR	1	37	30.175
THERMAL	ALUAR	1	140	27.6
THERMAL	C. RIVADAVIA A	1	16	30.7
THERMAL	C. RIVADAVIA A	1	25	30.475
THERMAL	C. RIVADAVIA A	1	22	30.55
THERMAL	C. RIVADAVIA A	1	23	30.525
THERMAL	C. RIVADAVIA A	1	23	30.525
THERMAL	C. RIVADAVIA A1	1	23	30.525
THERMAL	C.T. LOS PERALES	2	37	30.175
THERMAL	C.T. M. BEHR	12	1.4	31.065
THERMAL	C.T. M. BEHR	3	2.97	31.02575
THERMAL	EL HUEMUL	16	1.4	31.065
THERMAL	EL HUEMUL	7	1.4	31.065
THERMAL	EL HUEMUL	7	1.8	31.055
THERMAL	EL HUEMUL	3	1.8	31.055
THERMAL	MESETA ESPINOSA	6	1.4	31.065
THERMAL	P. TRUNCADO I	1	15	30.725
THERMAL	P. TRUNCADO I	1	20	30.6
THERMAL	P. TRUNCADO I	1	15	30.725
THERMAL	RIO CHICO	3	17	30.675
THERMAL	RIO CHICO	3	11	30.825
THERMAL	RIO CHICO	1	12	30.8
THERMAL	RIO CHICO	1	10	30.85
THERMAL	RIO GALLEGOS	8	1.5	31.0625
THERMAL	RIO TURBIO	2	120	28.1
WIND	ALUAR	1	50.4	29.94
WIND	ALUAR	1	61.2	29.67
WIND	ALUAR	1	45.6	30.06

(*continued on next page*)

Table A.4 (*continued*)

Source	Name	Number of units	Capacity (MW)	Unitary Cost (USD/MWh)
WIND	CHUBUT NORTE	1	28.35	30.49125
WIND	CT PATAGONIA	2	38.5	30.2375
WIND	CT PATAGONIA	1	60	29.7
WIND	DIADEMA I	1	6.3	31.0425
WIND	DIADEMA II	1	27.6	30.51
WIND	EL TORDILLO	2	1.6	31.16
WIND	GARAYALE	7	3.45	31.11375
WIND	LOMA BLANCA II	16	3.2	31.12
WIND	LOMA BLANCA IV	17	3	31.125
WIND	M. BEHR	1	99	28.725
WIND	P.E. BICENTENARIO	1	100	28.7
WIND	P.E. BICENTENARIO II	1	21.6	30.66
WIND	P.E. MADRYN I	1	71	29.425
WIND	P.E. MADRYN II	1	151.2	27.42
WIND	P.E. RAWSON I	27	1.8	31.155
WIND	P.E. RAWSON II	16	1.8	31.155
WIND	P.E. RAWSON III	12	2	31.15
HYDRO	AMEGHINO	2	23.4	9.915
HYDRO	FUTALEUFU	4	133	7.175

Table A.5
Power plant information. North-east Region (NEA). Based on [53].

Source	Name	Number of units	Capacity (MW)	Unitary Cost (USD/MWh)
BIOMASS	BSROTV	1	18	72
HYDRO	SALTITOS	1	1	10.475
HYDRO	URUGUAI	2	70	8.75
HYDRO	YACYRETá	20	155	6.625
THERMAL	A. DEL VALLE	12	1.25	31.08875
THERMAL	BARRANQUERAS	17	1.4	31.085
THERMAL	C. CORRIENTES	24	0.8	31.1
THERMAL	C.T. ALEM	18	1	31.095
THERMAL	C.T. FORMOSA	24	0.65	31.10375
THERMAL	C.T. FORMOSA II	12	2.5	31.0575
THERMAL	C.T. GARRUCHOS	1	37	30.195
THERMAL	C.T. LAS PALMAS	12	0.6	31.105
THERMAL	C.T. PASO DE LA PATRIA	21	0.3	31.1125
THERMAL	CHARATA I	4	0.8	31.1
THERMAL	CHARATA II	8	1.2	31.09
THERMAL	CHARATA III	8	1.2	31.09
THERMAL	GOYA	8	1	31.095
THERMAL	GOYA	3	1.2	31.09
THERMAL	ING. JUAREZ	5	1	31.095
THERMAL	ITATI	12	0.3	31.1125
THERMAL	ITATI	4	0.7	31.1025
THERMAL	JJ. CASTELLI	18	0.9	31.0975
THERMAL	LAGUNA BLANCA	5	0.8	31.1
THERMAL	LAGUNA BLANCA	4	1	31.095
THERMAL	OBERA	1	13	30.795
THERMAL	PAPEL MSIONERO	1	7	30.945
THERMAL	PAPEL MSIONERO	1	15	30.745
THERMAL	PCIA. ROCA	1	6	30.97
THERMAL	PCIA. SAENZ PEñA	18	0.8	31.1
THERMAL	PCIA. SAENZ PEñA II	32	0.6	31.105
THERMAL	PINDO ECOENERGIA	1	4	31.02
THERMAL	PIRANE	24	0.6	31.105
THERMAL	PIRANE	3	0.8	31.1
THERMAL	PIRAY	1	8.8	30.9
THERMAL	PIRAY	1	31	30.345
THERMAL	PLANTA CELULOSA	1	30	30.37
THERMAL	POSADAS	1	22	30.57
THERMAL	SAN MARTIN	16	1	31.095
THERMAL	SANTA ROSA	1	6	30.97
THERMAL	VILLA ANGELA	18	0.83	31.09925

Table A.6
Power plant information. Litoral Region (LIT). Based on [53].

Source	Name	Number of units	Capacity (MW)	Unitary Cost (USD/MWh)
THERMAL	BRIG. LOPEZ	1	280	24.27
THERMAL	C. DE GOMEZ NORTE	4	16	30.87
THERMAL	C. DEL URUGUAY	2	20	30.77
THERMAL	C. TIMBUES	2	292	23.97
THERMAL	C. TIMBUES	1	280	24.27
THERMAL	C. VUELTA DE OBLIGADO	2	290	24.02
THERMAL	C. VUELTA DE OBLIGADO	1	280	24.27
THERMAL	C.T. AVELLANEDA	4	1.5	31.2325
THERMAL	CERES	14	1.4	31.235
THERMAL	G. RENOVA	1	185	26.645
THERMAL	LA PAZ	9	1.2	31.24
THERMAL	M. RIO DE LA PLATA	1	25	30.645
THERMAL	PARANA ESTE	2	21.2	30.74
THERMAL	PEREZ	8	9.5	31.0325
THERMAL	RAFAELA OESTE	14	1.6	31.23
THERMAL	RUFINO	24	1.4	31.235
THERMAL	S.P. VERDE	1	1.4	31.235
THERMAL	SAN SALVADOR	9	1.2	31.24
THERMAL	SORRENTO	1	160	27.27
THERMAL	SULFACID	1	15	30.895
THERMAL	V. OCAMPO SUR	5	9.5	31.0325
THERMAL	VENADO TUERTO	14	1.5	31.2325
THERMAL	VIALE	12	0.8	31.25
HYDRO	SALTO GRANDE	7	135	9.65

Table A.7
Power plant information. Centro Region (CEN). Based on [53].

Source	Name	Number of units	Capacity (MW)	Unitary Cost (USD/MWh)
BIOMASS	PRODEMAN	1	10	076.50
BIOMASS	RIO IV DOS	1	1.2	078.70
BIOMASS	RIO IV UNO	2	1.2	078.70
BIOMASS	TICINO	1	4	078.00
WIND	ACHI	1	48	029.80
WIND	EL JUME	1	8	030.80
WIND	MANQ	1	57	029.58
WIND	OLIV	1	23	030.43
HYDRO	CASSAFFOUSTH	3	5.4	010.12
HYDRO	FITZ SIMONS	3	3.5	010.16
HYDRO	LA VIñA	2	7.5	010.06
HYDRO	LOS MOLINOS	4	14	009.90
HYDRO	LOS MOLINOS	1	4	010.15
HYDRO	P. MORAS	1	7.5	010.06
HYDRO	REOLIN	3	16	009.85
HYDRO	RIO GRANDE	4	185	005.63
HYDRO	SAN ROQUE	4	6.5	010.09
NUCLEAR	EMBALSE	1	648	027.68
SOLAR PV	CALO	1	17.5	030.78
SOLAR PV	CSOL	1	5	031.10
SOLAR PV	CUMB	1	22	030.67
SOLAR PV	CUMB 2	1	4	031.12
SOLAR PV	SPUN	1	5	031.10
THERMAL	13 DE JULIO	2	16	030.72
THERMAL	BELL VILLE	16	0.8	031.10
THERMAL	BELL VILLE	6	0.8	031.10
THERMAL	GRAL. LEVALLE	2	23	030.55
THERMAL	ISLA VERDE	24	0.85	031.10
THERMAL	MARANZANA I	2	35	030.25
THERMAL	MARANZANA II	3	60	029.62
THERMAL	MARANZANA II	2	50	029.87
THERMAL	OESTE	2	16	030.72
THERMAL	PILAR	2	157	027.20
THERMAL	PILAR	1	170	026.87
THERMAL	PILAR II	2	32	030.32
THERMAL	PILAR II	2	75	029.25
THERMAL	RIO III	1	60	029.62
THERMAL	SAN FRANCISCO	1	16	030.72
THERMAL	SAN FRANCISCO	1	23	030.55
THERMAL	SUROESTE	4	35	030.25
THERMAL	VILLA MARIA	4	49	029.90
THERMAL	VILLA MARIA	3	16	030.72
THERMAL	YANQUETRUZ	2	0.75	031.10

Table A.8
Power plant information. North-west Region (NOA). Based on [53].

Source	Name	Number of units	Capacity (MW)	Unitary Cost (USD/MWh)
THERMAL	AGUILARES	1	16.2	032.01
THERMAL	AñATUYA I	16	1.2	032.38
THERMAL	AñATUYA II	14	0.8	032.39
THERMAL	BANDERA	32	1	032.39
THERMAL	BRACHO	1	268	025.71
THERMAL	C. CORRAL	3	33	031.59
THERMAL	CAFAYATE	1	80	030.41
THERMAL	CAFAYATE	1	7	032.24
THERMAL	CAIMANCITO	5	18	031.96
THERMAL	CATAMARCA	15	1.6	032.37
THERMAL	CENTRAL REYES	2	4	032.31
THERMAL	FRIAS	1	60	030.91
THERMAL	INDEPENDENCIA	2	50	031.16
THERMAL	ING. GIAI	1	10	032.16
THERMAL	INTA	8	0.9	032.39
THERMAL	LA BANDA	2	13	032.09
THERMAL	LEALES	2	7.5	032.22
THERMAL	LEDESMA	14	0.6	032.40
THERMAL	LEDESMA	1	16	032.01
THERMAL	ORAN	14	1	032.39
THERMAL	P. INT CATAMARCA	12	1.3	032.38
THERMAL	PIQUIRENDA	10	3	032.34
THERMAL	PLUSPETROL NORTE	2	116	029.51
THERMAL	PUEBLO VIEJO	2	7.7	032.22
THERMAL	SAN JUANCITO	2	207	027.24
THERMAL	SAN JUANCITO	1	229	026.69
THERMAL	SAN MIGUEL DE TUC	1	165	028.29
THERMAL	SAN MIGUEL DE TUC	1	140	028.91
THERMAL	SAN MIGUEL DE TUC	1	124	029.31
THERMAL	TABACAL	1	38	031.46
THERMAL	TARTAGAL	1	14	032.06
THERMAL	TEREVINTOS	8	1	032.39
THERMAL	TINOGASTA	20	0.8	032.39
THERMAL	TINOGASTA	1	11	032.14
THERMAL	TINOGASTA	1	15	032.04
THERMAL	TINOGASTA	1	7	032.24
THERMAL	TUCUMAN	2	157	028.49
THERMAL	TUCUMAN	1	162	028.36
HYDRO	EL TUNAL	2	7	010.12
HYDRO	ESCABA	3	8	010.09
HYDRO	GUEMES	2	60	008.79
HYDRO	GUEMES	1	125	007.17
HYDRO	LAS MADERAS	2	15	009.92
HYDRO	LEDESMA	12	0.7	010.27
HYDRO	LEDESMA	1	20	009.79
HYDRO	LOS QUIROGA	2	1	010.27
HYDRO	R. HONDO	1	8	010.09
HYDRO	R. HONDO	1	9.5	010.05
SOLAR PV	CITRUSVIL	3	1.2	031.73
SOLAR PV	CORRALITO	2	8	031.56
SOLAR PV	EL CADILLAL	2	6	031.61
SOLAR PV	GUEMES	1	100	029.26
SOLAR PV	INDEPENDENCIA	2	60	030.26
SOLAR PV	SAUJIL	1	22.5	031.20

Table A.10
Power plant information. Comahue Region (COM). Based on [53].

Source	Name	Number of units	Capacity (MW)	Unitary Cost (USD/MWh)
THERMAL	AGUA DEL CAJóN	3	48	031.21
THERMAL	AGUA DEL CAJóN	2	45	031.29
THERMAL	AGUA DEL CAJóN	1	130	029.16
THERMAL	AGUA DEL CAJóN	1	270	025.66
THERMAL	ALTO VALLE	2	25	031.79
THERMAL	ALTO VALLE	1	17	031.99
THERMAL	ALTO VALLE	1	15	032.04
THERMAL	ALTO VALLE	1	15	032.04
THERMAL	ALUMINé	6	1.2	032.38
THERMAL	BARILOCHE	20	1	032.39
THERMAL	CAVIAHUE	7	1.2	032.38
THERMAL	CHIHUIDO	2	19.5	031.92
THERMAL	CIPOLETTI	6	0.8	032.39
THERMAL	ENTRE LOMAS 2	18	1.4	032.38
THERMAL	IMEXTRADE	1	6	032.26
THERMAL	LOMA CAMPANA	2	105	029.79
THERMAL	LOMA DE LA LATA	3	125	029.29
THERMAL	LOMA DE LA LATA	1	172	028.11
THERMAL	LOMA DE LA LATA	1	106	029.76
THERMAL	LOMA DE LA LATA	1	106	029.76
THERMAL	LOMITA	22	1	032.39
THERMAL	PLAZA HUINCUL	1	40	031.41
THERMAL	REALICó	20	1.8	032.37
THERMAL	RINCON DE LOS SAUCES	27	1.4	032.38
THERMAL	TERMO ROCA	1	133	029.09
THERMAL	TERMO ROCA	1	60	030.91
THERMAL	USINA CAMPAMENTO	4	5.1	032.28
THERMAL	USINA EL TRAPIAL	3	5.1	032.28
THERMAL	USINA EL TRAPIAL	1	3	032.34
HYDRO	ALICURá	4	250	010.19
HYDRO	ARROYITO	3	40	010.22
HYDRO	CASA DE PIEDRA	2	30	010.24
HYDRO	CIPOLETTI	1	5.7	010.27
HYDRO	DIVISADEROS	2	5	010.24
HYDRO	EL CHOCóN	6	200	010.14
HYDRO	GRAL. ROCA	1	1	010.27
HYDRO	J. ROMERO	2	2.4	010.24
HYDRO	PICHI PICUN LEUFU	3	80	010.22
HYDRO	PIEDRA DEL AGUILA	4	350	010.19
HYDRO	R. ESCONDIDO	6	1.2	010.14
HYDRO	RIO COLORADO	2	2.7	010.24
HYDRO	SALTO ANDERSEN	2	3.8	010.24
WIND	BAJADA COLORADA	1	100	029.26
WIND	LA BANDERITA	1	36.75	030.84
WIND	PLANICIE BANDERITA	2	225	026.14
WIND	POMONA	29	3.9	031.66

Table A.11
Power plant information. Cuyo Region (CUY). Based on [53].

Source	Name	Number of units	Capacity (MW)	Unitary Cost (USD/MWh)
THERMAL	ANCHORIS	4	10	032.16
THERMAL	CHILECITO	1	1.2	032.38
THERMAL	LA RIOJA	9	1.1	032.38
THERMAL	LA RIOJA	3	13	032.09
THERMAL	LA RIOJA	1	50	031.16
THERMAL	LA RIOJA NORTE 2	1	22.4	031.85
THERMAL	LUJAN DE CUYO	2	60	030.91
THERMAL	LUJAN DE CUYO	2	45	031.29
THERMAL	LUJAN DE CUYO	1	85	030.29
THERMAL	LUJAN DE CUYO	1	200	027.41
THERMAL	LUJAN DE CUYO	1	28	031.71
THERMAL	LUJAN DE CUYO	1	25	031.79
THERMAL	LUJAN DE CUYO	1	23	031.84
THERMAL	MALLIGASTA	1	5	032.29
THERMAL	MALLIGASTA	1	8	032.21
THERMAL	SARMIENTO	3	10	032.16
HYDRO	A. CONDARCO	2	14.8	009.92
HYDRO	A. CONDARCO	1	25	009.67
HYDRO	AGUA DEL TORO	2	75	008.42
HYDRO	C.H.S. MARTIN	3	2	010.24
HYDRO	CACHEUTA	4	30	009.54
HYDRO	CARACOLES	2	60.7	008.77
HYDRO	CUESTA DEL VIENTO	1	8	010.09
HYDRO	EL CARRIZAL	2	8	010.09
HYDRO	EL TIGRE	2	7	010.12
HYDRO	H. ULLUM	2	22.5	009.73
HYDRO	LOS CORONELES	2	3.32	010.21
HYDRO	LOS REYUNOS	2	112	007.49
HYDRO	LUNLHI	2	4.14	010.19
HYDRO	NIHUIL I	4	20	009.79
HYDRO	NIHUIL II	4	18	009.84
HYDRO	NIHUIL II	2	19	009.82
HYDRO	NIHUIL III	2	22	009.74
HYDRO	NIHUIL IV	1	26	009.64
HYDRO	PUNTA NEGRA	2	31.6	009.50
HYDRO	QUEBRADA DE ULLUM	1	45	009.17
HYDRO	TBENHI	2	0.8	010.27
WIND	ARAUCO	2	25	031.14
WIND	ARAUCO II	1	100	029.26
SOLAR PV	ANPCFV	1	3	031.69
SOLAR PV	CHEPES	1	2	031.71
SOLAR PV	DIAGUITAS	1	1.8	031.72
SOLAR PV	GUAñIZUIL	1	80	029.76
SOLAR PV	LAS LOMITAS	1	2	031.71
SOLAR PV	LOS LLANOS	1	12	031.46
SOLAR PV	NONOGASTA	1	35	030.89
SOLAR PV	P.S. PASIP	1	1.5	031.72
SOLAR PV	SOLAR DE LOS ANDES	1	5	031.64
SOLAR PV	SOLAR ULLUM	2	25	031.14
SOLAR PV	SOLAR ULLUM	1	32	030.96
SOLAR PV	SOLAR ULLUM	1	13.5	031.42
SOLAR PV	SOLAR ULLUM	1	6.5	031.60

Credit author statement

Gonzalo Alvarez: Conceptualization, Methodology, Software, Data collection, Writing- Original draft preparation, Visualization, Investigation, Supervision, Validation, Writing- Reviewing and Editing.

Funding

The author received no specific funding for this work.

References

[1] Nacoti M, Ciocca A, Giupponi A, Brambillasca P, Lussana F, Pisano M, et al. At the epicenter of the covid-19 pandemic and humanitarian crises in Italy: changing perspectives on preparation and mitigation. Catal Non-Issue Content 2020. https://doi.org/10.1056/CAT.20.0080.
[2] Nicola M, Alsafi Z, Sohrabi C, Kerwan A, Al-Jabir A, Iosifidis C, et al. The socio-economic implications of the coronavirus pandemic (COVID-19): a review. Int J Surg 2020. https://doi.org/10.1016/j.ijsu.2020.04.018.
[3] Alvarez GE. Optimization analysis for hydro pumped storage and natural gas accumulation technologies in the Argentine Energy System. J Energy Storage 2020;31:101646. https://doi.org/10.1016/j.est.2020.101646.
[4] Andruszkiewicz J, Lorenc J, Weychan A. Seasonal variability of price elasticity of demand of households using zonal tariffs and its impact on hourly load of the power system. Energy 2020;196:117175. https://doi.org/10.1016/j.energy.2020.117175.

[5] Franco G, Sanstad AH. Climate change and electricity demand in California. Climatic Change 2008;87:139–51. https://doi.org/10.1007/s10584-007-9364-y.
[6] Halicioglu F. Residential electricity demand dynamics in Turkey. Energy Econ 2007;29:199–210. https://doi.org/10.1016/j.eneco.2006.11.007.
[7] Thatcher MJ. Modelling changes to electricity demand load duration curves as a consequence of predicted climate change for Australia. Energy 2007;32:1647–59. https://doi.org/10.1016/j.energy.2006.12.005.
[8] Zhou C, Su F, Pei T, Zhang A, Du Y, Luo B, et al. COVID-19: challenges to GIS with big data. Geogr Sustain 2020;1(1):77–87. https://doi.org/10.1016/j.geosus.2020.03.005.
[9] Folgueira MD, Munoz-Ruiperez C, Alonso-Lopez MA, Delgado R. SARS-CoV-2 infection in health care workers in a large public hospital in Madrid, Spain, during March 2020. 2020. https://doi.org/10.1101/2020.04.07.20055723.
[10] Salmeron J, Wood K, Baldick R. Analysis of electric grid security under terrorist threat. IEEE Trans Power Syst 2004;19:905–12. https://doi.org/10.1109/TPWRS.2004.825888.
[11] Arroyo JM, Galiana FD. On the solution of the bilevel programming formulation of the terrorist threat problem. IEEE Trans Power Syst 2005;20:789–97. https://doi.org/10.1109/TPWRS.2005.846198.
[12] Gusrialdi A, Qu Z. Smart grid security: attacks and defenses. Smart grid control. Power electron. Power Syst. Cham: Springer; 2019. p. 199–223. https://doi.org/10.1007/978-3-319-98310-3_13.
[13] Wang X, Virguez E, Xiao W, Mei Y, Patiño-Echeverri D, Wang H. Clustering and dispatching hydro, wind, and photovoltaic power resources with multi-objective optimization of power generation fluctuations: a case study in southwestern China. Energy 2019;189:116250. https://doi.org/10.1016/j.energy.2019.116250.
[14] El Sehiemy RA, Selim F, Bentouati B, Abido MA. A novel multi-objective hybrid particle swarm and salp optimization algorithm for technical-economical-environmental operation in power systems. Energy 2020;193:116817. https://doi.org/10.1016/j.energy.2019.116817.
[15] Marler RT, Arora JS. Survey of multi-objective optimization methods for engineering. Struct Multidiscip Optim 2004;26:369–95. https://doi.org/10.1007/s00158-003-0368-6.
[16] Kuloor S, Hope GS, Malik OP. Environmentally constrained unit commitment. IEE Proc C Gener Transm Distrib 1992;139:122. https://doi.org/10.1049/ip-c.1992.0020.
[17] Bath SK, Dhillon JS, Kothari DP. Fuzzy satisfying stochastic multi-objective generation scheduling by weightage pattern search methods. Elec Power Syst Res 2004;69:311–20. https://doi.org/10.1016/j.epsr.2003.10.006.
[18] Reza Norouzi M, Ahmadi A, Esmaeel Nezhad A, Ghaedi A. Mixed integer programming of multi-objective security-constrained hydro/thermal unit commitment. Renew Sustain Energy Rev 2014;29:911–23. https://doi.org/10.1016/j.rser.2013.09.020.
[19] Mavrotas G. Generation of efficient solutions in Multiobjective Mathematical Programming problems using GAMS. Effective implementation of the ε-constraint method. Zografou Campus, Athens; 2007. 15780, Greece.
[20] Parvizi M, Shadkam Elham, jahani Niloofar. A hybrid COA/ε-constraint method for solving multi-objective problems. Int J Found Comput Sci Technol 2015;5:14.
[21] Simoglou CK, Biskas PN, Bakirtzis AG. Optimal self-scheduling of a thermal producer in short-term electricity markets by MILP. IEEE Trans Power Syst 2010;25. https://doi.org/10.1109/TPWRS.2010.2050011. 1965–77.
[22] Li X, Li T, Wei J, Wang G, Yeh WWG. Hydro unit commitment via mixed integer linear programming: a case study of the three gorges project, China. IEEE Trans Power Syst 2014;29:1232–41. https://doi.org/10.1109/TPWRS.2013.2288933.
[23] Chen CH, Chen N, Luh PB. Head dependence of pump-storage-unit model applied to generation scheduling. IEEE Trans Power Syst 2017;32:2869–77. https://doi.org/10.1109/TPWRS.2016.2629093.
[24] Lima RM, Grossmann IE. Computational advances in solving mixed integer linear programming problems. Chem Eng Greetings to Prof Sauro Pierucci Occas His 65th Birthd 2011:151–60.
[25] Alvarez GE. Operation of pumped storage hydropower plants through optimization for power systems. Energy 2020;202:117797. https://doi.org/10.1016/j.energy.2020.117797.
[26] Breeze P. Power generation technologies. second ed. Elsevier; 2014. https://doi.org/10.1016/C2012-0-00136-6.
[27] Zhao J, Tang YH, Wang L, Liu DC. The balance of power system peak load regulation considering the participation of nuclear power plant. Appl Mech Mater 2014;672–674:477–81. https://dx.doi.org/10.4028/www.scientific.net/amm.672-674.477.
[28] Nuclear Energy Agency. Technical and economic aspects of load following with nuclear power plants. 2011.
[29] Alvarez GE. Integrated scheduling from a diversity of sources applied to the Argentine electric power and natural gas systems. Comput Chem Eng 2020;134:106691. https://doi.org/10.1016/j.compchemeng.2019.106691.
[30] Stott B, Jardim J, Alsac O. DC power flow revisited. IEEE Trans Power Syst 2009;24:1290–300. https://doi.org/10.1109/TPWRS.2009.2021235.
[31] Yuan X, Zhang B, Wang P, Liang J, Yuan Y, Huang Y, et al. Multi-objective optimal power flow based on improved strength Pareto evolutionary algorithm. Energy 2017;122:70–82. https://doi.org/10.1016/j.energy.2017.01.071.
[32] Mazidi M, Monsef H, Siano P. Design of a risk-averse decision making tool for smart distribution network operators under severe uncertainties: an IGDT-inspired augment ε-constraint based multi-objective approach. Energy 2016;116:214–35. https://doi.org/10.1016/j.energy.2016.09.124.
[33] Ahmadi A, Aghaei J, Shayanfar HA, Rabiee A. Mixed integer programming of multiobjective hydro-thermal self scheduling. Appl Soft Comput 2012;12:2137–46. https://doi.org/10.1016/j.asoc.2012.03.020.
[34] Mavrotas G. Effective implementation of the ε-constraint method in multi-objective mathematical programming problems. Appl Math Comput 2009;213:455–65. https://doi.org/10.1016/j.amc.2009.03.037.
[35] Donateo T, Serrao L, Rizzoni G. A two-step optimisation method for the preliminary design of a hybrid electric vehicle. Int J Electr Hybrid Veh 2008;1:142. https://doi.org/10.1504/IJEHV.2008.017831.
[36] Osorio Muriel AF, Brailsford S, Smith H. A bi-objective optimization model for technology selection and donor's assignment in the blood supply chain. Sist y Telemática 2014;12:9. https://doi.org/10.18046/syt.v12i30.1854.
[37] Zykina AV. A lexicographic optimization algorithm. Autom Rem Contr 2004;65:363–8. https://doi.org/10.1023/B:AURC.0000019366.84601.8e.
[38] Madurai Elavarasan R, Pugazhendhi R. Restructured society and environment: a review on potential technological strategies to control the COVID-19 pandemic. Sci Total Environ 2020;725:138858. https://doi.org/10.1016/j.scitotenv.2020.138858.
[39] Javaid M, Haleem A, Vaishya R, Bahl S, Suman R, Vaish A. Industry 4.0 technologies and their applications in fighting COVID-19 pandemic. Diabetes Metab Syndr Clin Res Rev 2020;14:419–22. https://doi.org/10.1016/j.dsx.2020.04.032.
[40] Staszkiewicz P, Chomiak-Orsa I, Staszkiewicz I. Dynamics of the COVID-19 contagion and mortality: country factors, social media, and market response evidence from a global panel analysis. IEEE Access 2020;8:106009–22. https://doi.org/10.1109/ACCESS.2020.2999614.
[41] De Dicco R. Indicadores Sector Eléctrico de Argentina. San Carlos de Bariloche; 2014.
[42] General Algebraic Modeling System (GAMS). GAMS Development 2016.
[43] IBM ILOG CPLEX Optimizer. Version 12.3.0.0. Jul 2011. 20AD.
[44] Grey A, Sekar A. Unified solution of security-constrained unit commitment problem using a linear programming methodology. IET Gener Transm Distrib 2008;2:856–67. https://doi.org/10.1049/iet-gtd.
[45] CAMMESA. Base generators 2020:1. accessed May 23, 2020, https://portalweb.cammesa.com/memnet1/revistas/estacional/base_gen.html.
[46] CAMMESA. Demanda real del SADI y regionales. Inf Oper 2020. https://portalweb.cammesa.com/default.aspx. [Accessed 22 April 2020].
[47] CAMMESA MEM. Demand Evolution Demand. Impact of DNU 297/20. Preventive and obligatory social isolation. Buenos Aires: Quarantine effect; 2020.
[48] CAMMESA. Main variables of the month. Monthly report. July 2020. Buenos Aires. 2020.
[49] CAMMESA. COVID-19 electricity demand behaviour in the MEM (in Spanish). COVID-19 Rep. 2020. accessed August 19, 2020, https://portalweb.cammesa.com/Pages/comdemcovid19.aspx.
[50] Presidency of Argentina. Novel COVID-19. Buenos Aires: Daily Report; 2020.
[51] U.S. BUREAU OF LABOR STATISTICS. Power plant operators, distributors, and dispatchers. Occup Outlook Handb > Prod. 2020. accessed August 18, 2020, https://www.bls.gov/OOH/production/power-plant-operators-distributors-and-dispatchers.htm.
[52] FREBA. Informe del sector eléctrico de la Provincia de Buenos Aires. 2019.
[53] CAMMESA. Unifilares de la Red eléctrica. Informes 2021:3. accessed February 22, 2021, https://portalweb.cammesa.com/Pages/Informes/EsquemasUnifilaresRedElectrica.aspx.